The Effect of Burning on Pre-incineration Trauma in Bone

by

Enya Kuan-Han Chang

(CHNENY001)

SUBMITTED TO THE UNIVERSITY OF CAPE TOWN

In partial fulfillment of the requirements for the degree

MPhil (Biomedical Forensic Science)

Division of Forensic Medicine and Toxicology

Faculty of Health Sciences

UNIVERSITY OF CAPE TOWN

03 April 2023

Supervisor: Mr. Calvin Mole

Co-supervisor: Dr. Shameemah Abrahams

DECLARATION

I, *Enya Kuan-Han Chang*, hereby declare that the work on which this dissertation is based is my original work (except where acknowledgements indicate otherwise) and that neither the whole work nor any part of it has been, is being, or is to be submitted for another degree in this or any other university. I authorise the university to reproduce for the purpose of research either the whole or any portion of the contents.

This thesis/dissertation has been submitted to the Turnitin module (or equivalent similarity and originality checking software) and I confirm that my supervisor has seen my report and any concerns revealed by such have been resolved with my supervisors in any manner whatsoever.

I have followed the referencing style according to the Harvard referencing style. Each significant contribution to, and quotation in, this dissertation from the work, or works of other people has been attributed, cited, and referenced.

Name: Enya Kuan-Han Chang

Student number: CHNENY001 (1513601)

Signature: Signed by candidate

Date: 03 April 2023

ABSTRACT

The act of burning is a common method of destroying and concealing evidence which may include dismemberment of the body. Saws used during dismemberment leave characteristic marks on bone, the analysis of which can assist in forensic casework. Research that has been conducted to date, provide minimal information on controlled temperatures to analyse and distinguish pre- and post-burning trauma marks. The aim of this research was to assess and compare morphological differences of pre-existing bone trauma before and after burning at various controlled temperatures. In this research, a back saw (tenon saw) was used to manually inflict trauma on de-fleshed *Ovis aries* femur bones (n = 18). These bones were later exposed to heat at controlled temperatures of 400°C, 600°C and 800°C for 20 minutes. Three different cut marks including a shallow false start, incomplete cut and a complete transection of the bone were inflicted on the mid-shaft of each bone specimen through which 54 lesions were analysed. Differences in saw mark characteristics of the cut surfaces before and after exposure to heat were investigated and compared. The following characteristics were examined: blade drift, bone islands, breakaway spurs, exit chipping, harmonics, kerfs, pull-out striae, striation regularity, tooth hop and profile shape. Quantitative analyses were conducted using macroscopic techniques and stereomicroscope to examine the specific characteristics of the different saw marks. All pre-existing trauma except one cut mark (shallow false start) survived after the burning process. The shallow false start was lost during the burning process and could not be recovered. The saw marks were distinguishable from heat-related fractures in all temperature groups. In some cases, characteristics such as exit chipping, pull-out striae and striation regularity were enhanced post-burning. Nonetheless, the post-burning survival and detection of saw marks can be obscured which may affect the visibility of sharp force trauma. Therefore, additional research for instance burning the bones at different durations and increasing the sample size should be examined. Furthermore, information on other factors and variables such as bone type or burning environment can be collected to create a database to increase accuracy of saw mark analysis.

Acknowledgements

Firstly, I am extremely grateful to my supervisor, Calvin Mole, for his invaluable supervision and patience during my research project. He is always available to provide answers and assistance no matter the time and day.

I would also like to thank every individual at the Forensic Medicine and Toxicology department who assisted me and for their insightful comments and suggestions.

Additionally, I would like to offer my special thanks to the University of Cape Town Postgraduate Funding Office (PGFO) and the National Research Foundation (NRF) for funding.

I am deeply thankful for my family, especially my parents for allowing me to do what I am most passionate about and always providing the love, care and need during this time.

Lastly, my gratitude extends to my friends and close people who contributed where they can at every stage of the research. They showed unwavering support, motivation, encouragement and believed in me throughout my academic journey.

Table of Contents

DECLARATION I
ABSTRACT II
Acknowledgements III
List of Figures VI
List of Tables VII
List of Abbreviations VIII
CHAPTER 1: Literature Review 1
Introduction 1
1.1 Saw mark characteristics 2
1.1.1 False start lesions: striation patterns and teeth per inch (TPI) in saws 4
1.1.2 Methods for analysing saw mark trauma 7
1.2 Heat-induced alterations to bone 8
1.2.1 Bone structure and composition 8
1.2.2 Heat-induced alteration to bone 8
1.3 Heat-induced alteration of pre-existing saw marks 12
1.3.1 Open air experiments 12
1.3.2 Furnace experiments 14
1.4 Conclusion 17
Aim of Study 18
Hypotheses 18
CHAPTER 2: Materials and Methods 19
2.1 Specimens 19
2.2 Saw mark trauma 19
2.3 Burning 21
2.4 Saw mark characteristics 21
2.5 Data Analysis 23
2.5.1 Inter/intra-observer error 24
2.6 Ethical clearance 24
CHAPTER 3: Results 25
3.1 Observer error results 25
3.1.1 Inter-observer 25
3.1.2 Intra-observer 25
3.2 Discolouration, fragmentation/fractures and weight 26
3.3 False start lesions 29

3.3.1 Kerf width & kerf depth 29
3.3.2 Blade drift & bone islands 31
3.3.3 Profile shapes 31
3.4 Incomplete cuts/lesions 33
3.4.1 Kerf width & kerf depth 33
3.4.2 Exit chipping, harmonics & bone islands 36
3.4.3 Profile shapes 36
3.5 Complete transections 37
3.5.1 Breakaway spurs 37
3.5.2 Pull-out striae 38
3.5.3 Striations regularity 39
3.5.4 Exit chipping, harmonics and tooth hops 40
CHAPTER 4: Discussion 44
4.1 Experimental design and conditions 45
4.2 Casts 46
4.3 Thermal alteration: colouration and fractures 47
4.4 Thermal alteration: saw mark characteristics 49
4.5 Limitations, improvements and future research 52
Conclusion 53
References 55
APPENDIX A: Summary Table of Thermal Alteration on Pre-existing Trauma on Bone i
APPENDIX B: Bone Biomechanics Measurements iii
APPENDIX C: Ethics Approval Letter iv
APPENDIX D: Heat-induced Fractures and Colouration of Bones vi
APPENDIX E: Bone Weight Before and After Burning vii
APPENDIX F: Additional Visualisation Methods viii
F1. Silicone casting method viii
F2. Fingerprint powder method ix
APPENDIX G: Measurements of Saw Mark Characteristics x
APPENDIX H: Saw Mark Data Collection (Meta-data) xix

List of Figures

Figure 1: 13 TPI backsaw used in the study. 20
Figure 2: Mitre block secured with G-clamps. 20
Figure 3: Different cut types inflicted onto the mid-shaft of femur bone. A) Complete transection, B) Shallow false start lesions and C) Incomplete cut/deep false start.....21
Figure 4: Bones burnt at various controlled degrees. A) 400°C, B) 600°C and C) 800°C.....27
Figure 5: Heat-induced fracture (green arrow) originating from the incomplete cut (at 800°C) and can be differentiated from saw mark (red arrow).....28
Figure 6: The kerf width of false start in A) unburnt and B) burnt bone.....30
Figure 7: Box plots of false starts mean kerf widths (millimetres) before and after burning in each burn temperature group. 30
Figure 8: Box plots of false start kerf depths (millimetres) before and after burning in each burn temperature group. Only one false start could be recovered in the 800°C burn group; thus, no accurate results are shown.....31
Figure 9: Profile shapes of false starts. A) Round shape and B) square with round corner shape. 32
Figure 10: Box plots of incomplete cut mean kerf widths (millimetres) before and after burning in each burn temperature group.....34
Figure 11: The kerf depth of incomplete lesions in A) unburnt and B) burnt bone. 35
Figure 12: Box plots of incomplete cut kerf depths (millimetres) before and after burning in each burn temperatures groups. 35
Figure 13: The breakaway spur of a complete cut on A) unburnt and B) burnt bone. 38
Figure 14: Pull-out striae before burning.....39
Figure 15: Pull-out striae after burning.....39
Figure 16: Box plots of mean striation distance (millimetres) of complete cuts before and after burning in each burn temperatures groups. 40
Figure 17: Exit chipping identified on a complete cut of a burnt bone. 41
Figure 18: Tooth hop present on bone before burning. 42
Figure 19: Tooth hop absent on bone after burning.....42

List of Tables

Table 1: Saw mark characteristic definitions derived from Symes et al. (2010); Martlin & Rando (2020) and Nogueira et al. (2016). 6
Table 2: Definition of most common fracture types (Derived from Herrman & Bennet, 1999; Mata-Tutor et al., 2021a; and Symes et al., 2008). 11
Table 3: Criteria for the analysis of various cut types for pre- and post-incineration of bone specimens. 23
Table 4: Intraclass correlation results of numerical variables for inter-observer. 25
Table 5: Intraclass correlation results of numerical results for intra-observer. 26
Table 6: Fracture types in different temperature groups. 29
Table 7: Mean measurement and presence of saw characteristics of false start lesions. 33
Table 8: Mean measurement and presence of saw characteristics of incomplete cuts. 37
Table 9: Mean measurement and presence of saw characteristics of complete transections... 43

List of Abbreviations

AP: Anterior-posterior

ICC: Intraclass correlation

I: Moment of inertia

ML: Medial-lateral

PPI: Points per inch

SD: Standard deviation

SM: Stereomicroscope

SEM: Scanning electron microscope

TPI: Teeth per inch

CHAPTER 1: Literature Review

Introduction

Burn injuries commonly occur from fire outbreaks and exposure to ultraviolet radiation, radioactivity, electricity as well as chemicals. The World Health Organisation reported the global death rate caused by burns are estimated to be 195 000 annually (WHO, n.d.), with Africa having one of the highest mortality rates due to fire-related injuries. In a study by Van Niekerk, Laubscher & Laflamme (2009), it was found Cape Town, South Africa had a burn mortality rate of 7.9 per 100 000 person years in the period of 2001 to 2004. Burn risks are often correlated to socioeconomic status (WHO, 2018). Although more than 95% of fatal fire-related burns occur within low- and middle-income countries, fire outbreaks and burns are often overlooked as a public health concern, despite being preventable by individuals and societies.

In South Africa, house fires, open nature fires and fires in informal settlements are common occurrences. The primary contributors to the outbreak and spread of fires are paraffin stoves, kerosene lamps and cooking fires, which are frequently used for cooking, warmth and light in the lower socio-economic population. Most fire-related fatalities are accidental and tend to occur outdoors or in vehicles. On the other hand, cases of criminal burning and rare cases of self-immolation as a means of suicide, occur most frequently indoors, in correspondence with the victim's homes (Blom, Van Niekerk & Laflamme, 2011; Fanton et al., 2006). Although most fire-related deaths are acidental, the intentional use of fire to conceal a victim's identity or destroy evidence of a crime should not be overlooked (Ubelaker, 2009).

The presence of post-mortem burning should be focused on as it may indicate that homicide has occurred (Mata-Tutor et al., 2021a). Various factors and identifying characteristics surrounding a burned body may help indicate that a homicide took place, and that fire was used to conceal the crime. Possible factors include accelerants that may be present on the body, various violent marks or injuries, and the absence of any vital signs. These are usually observed through medico-legal autopsy and investigations. It is critical to determine whether or not the victim(s) was exposed to fire before or after burning along with other injuries that may be found (Tümer et al., 2012).

Hidden fractures or injuries may not always be visible to the eye; therefore, radiography is often used to identify potential skeletal injuries which could suggest factors contributing to or

being the cause death (Fanton et al., 2006; Tümer et al., 2012). The biomechanical properties of bone are significantly different in fresh bone compared to burnt bone making it possible to distinguish perimortem fractures from heat-induced fractures and alteration (Herrman & Bennet, 1999; Keys & Ross, 2022; Krap et al., 2022; Mata-Tutor et al., 2021a; Pope & Smith, 2004).

It has also been established that dismemberment prior to burning is a common method of body disposal (Hughes, 2018; Keys & Ross, 2022; Mata-Tutor et al., 2021b). Dismemberment is the purposeful division of a body using sharp tools, typically in an act to disfigure an individual, impede identification, or to ease disposal of the body (Hackman & Black, 2017; Hughes, 2018; Martlin & Rando, 2020; Saville, Hainsworth & Rutty, 2007; Symes et al., 2010). Saws and knives leave characteristic tool marks on bone; however, further research is necessary to establish the degree of change associated with these characteristics following burning.

To thoroughly investigate cases involving burning it is necessary to understand how fire reacts in various setting, how this may affect the body, the effect of heat-induced changes of bone structure and how this may alter pre-existing injury. The following review will provide relevant information on characteristics of dismemberment and saw marks on bone, and macroscopic heat-induced changes to bone. Following this, the current state of information relating to heat-induced alteration of saw marks is presented.

1.1 Saw mark characteristics

Several authors have described the characteristics of sharp force trauma including saw marks on bone. Most characteristics assist with identifying the class of instrument used rather than individual identifiable features. Symes (1992) provides a thorough summary of these characteristics. In the context of forensic science, the characteristics of the tool can help identify and match to the sharp force trauma found on the victim's wounds and thereby lead to the classification of the murder weapon (Waltenberger & Schutkowski, 2017).

Saw mark morphology is dependent on several factors, including the type of blade used, the direction of cut, the power/speed exerted by humans, the strength of the individual as well as the skill to handle the saw (Symes et al., 2010). Manual infliction has shown that despite attempts to replicate the same angle and force per each action, various shapes and sizes of cut marks can be observed even when the same tool or weapon is used (Vachirawongsakorn, Painter & Márquez-Grant, 2022). Even though the cut marks vary, this might imply a natural

course of hand motion with blade interaction between different bones (Vachirawongsakorn, Painter & Márquez-Grant, 2022). This can be a valuable factor to identify the perpetrator's handedness.

In cases of dismemberment whereby limbs are severed from the body, it is crucial to analyse and identify the marks present (Waltenberger & Schutkowski, 2017). Three forms of cut may be apparent on the bone surface, namely false start lesions, incomplete cuts and full transection of bone. All these forms are defined by the creation of a kerf which retain toolmarks either on the floor or wall of the kerf. These saw marks on bones are created from saws that have a metallic part on which teeth are moved in a backwards and forwards motion. This motion can either be produced by hand or alternatively by power, using mechanical or electrical saws (Nogueira et al., 2016). Mechanical powered saws differ greatly from hand saws. Despite the fact, there have previously been multiple dismemberment and mutilation cases which were misinterpreted for the use of mechanical saws, when in fact hand saws were used (Symes et al., 2010).

All saws create kerfs; however, it is the variation in morphological surfaces or cross-sectional shape of the kerf that provides detail to assist in differentiate the class of blade being used (Dittmar, 2017) (Table 1). There are three different sets of blades that produce various saw marks. The first and most commonly found is the alternate set. This set shows each tooth that are alternately bent right and left throughout the blade; therefore, a tooth enters the bone material in an opposite direction each time. Another set is known as the wavy set. Such a tooth set has a slow alteration of tooth angle creating a wavy-like appearance of the teeth. The last set is known as the raker set, which includes an unset (or untangled) tooth followed by alternately set teeth, to ultimately create a different kerf pattern (Guilbeau, 1989; Symes et al., 2010).

Kerf floors are important in saw mark analysis as they provide information on the saw teeth and how far the tooth points are from each other (indicating the number of teeth per inch [TPI]). The shape of the kerf floor can be V-shaped (especially by knives), while the majority of saws with slightly broader blades, create U-shaped or W-shaped floors (Symes, 2010). Through the cutting process, saw teeth leave striations on the kerf wall which provide similarly valuable information relating to the power and direction of the cut (Symes et al., 2010; Robbins, Fairgrieve & Oost, 2014).

The kerf wall is made up of fine lines or furrows and striations which are created by the action of the saw teeth cutting through the bone. The pull stroke creates furrows while the forward stroke creates striations. The estimated stroke action may be calculated from the furrows and striations observed in the kerf wall. A distinct vertical mark called pull-out stria can be observed due to the saw blade being removed by a stroke that was stuck. These distinct vertical marks may give an indication of the tooth length and distance between teeth. Wave formation, also known as harmonics, exists as a result of the stopping and resuming motion when sawing. In addition, tooth hops are visible crests or peaks and valleys that can represent the distances between the individual teeth on the saw (Feldman, 2015; Saville, Hainsworth & Rutty, 2007; Symes et al., 2010).

In cases of complete transection of a bone, a kerf floor is obviously not present. However, as the bone is being sawed, bone projections may be formed at the most distal point of the cut direction. These projections are known as breakaway spurs and occur due to the propensity of bone to break prior to complete transection (Symes et al., 2010). Breakaway spurs often occur when sawing or cutting through bone using hand tools. The weight of the bone in relation to the action of sawing results in the bone breaking or snapping near the end of a complete transection (Bernardi et al., 2020; Robbins, Fairgrieve & Oost, 2014). Breakaway spurs may retain remnants of the kerf floor and should be thoroughly inspected.

1.1.1 False start lesions: striation patterns and teeth per inch (TPI) in saws

False start lesions as described by Nogueira et al. (2018) is a ‘superficial blade bite’ that can be found on the bone. In other words, the saw glides over the surface of the bone without cutting through it entirely (Bernardi et al., 2020). Saw marks can appear at different depths – the examination of incomplete saw marks and/or false start analysis created on bones has potential information on the saw type that created the marks (Alsop et al., 2020).

Alsop et al. (2020) used random forest plots from data obtained from micro-CT scans to show that the teeth set on saws as well as the different thickness of the blades, can be determined from the analysis of false start lesions. This assists to establish the type of saw that is used to create the false start lesions. In relation to casework, especially in dismemberment investigations, the false start lesions found on bones can tie into research findings and thereby help provide valuable insight into saw mark analysis.

In analysing false start lesions, secondary features may also be observed to classify the class of saws. Striations are macroscopically fine lines that are visible after a saw action is produced. The striations marks/patterns are a good indicator of direction of saw movement as well as the type of saw being used (Dittmar, 2017). The potential of finding striae on kerf walls decreases as the process of cutting through bone incurs wear changes. In other words, the blade/teeth of a sharp tool lose its sharpness while cutting through bone (Freas, 2010). Freas (2010) also mentioned that although wear-related characteristics can be found when experimentation takes place, these do not necessarily affect the process of identifying the saw class features, if the purpose of the investigation was to identify the tool used to inflict marks on bones.

Patterns of the striae on the kerf floor can appear to be undulating, undulating/straight or thin/straight depending on the type of blade set used to create the false start lesion. The results showed that the striae pattern that appeared to be undulating and undulating/straight were alternating blade set, while the thin/straight were the wavy blade set. Therefore, it was found that striated patterns found on the kerf floor are most useful saw class classification, whereas bone islands and blade drifts can be used to analyse the tooth per inch and the strength of the teeth (Nogueira et al., 2018; Symes, 1992).

The shape of the kerf wall/edges are also features that can be examined. The shapes can be used to denote the type of blade set that was used. Shapes which appear to be narrow and wide are often associated with alternating sets, while straight walls are more intricate to identify, as they can be linked to the raker set, as well as the alternating and wavy set. Lastly, the necking shape can be associated with the wavy set (Nogueira et al., 2016).

The striae that present peaks and valleys (observed as waves), are known as tooth hops. The mechanism of the formation of tooth hops is not fully understood. Symes (1992) suggests that tooth hop is the manifestation of a floor dip. Furthermore, the presence of tooth hops appears to be random with significant differences noted in the number of tooth hop present between samples and even between kerf walls of the same cut (Grosso, 2022). Nevertheless, tooth hops are an indication of the spacing of saw teeth through which TPI are measured. When observing a saw blade, TPI describes the number of teeth found per inch on the blade (Pelletti et al., 2017; Saville, Hainsworth & Rutty, 2007; Symes et al., 2010).

TPI is the measurement of complete teeth found on the saw per inch. Points per inch (PPI) has usually one more point than TPI but essentially makes up TPI and is the term universally used. The tooth that enters the bone material can indicate the direction and can provide the distance

between the tooth which eventually leads to calculating the TPI. TPI dictates the saw size and can be extracted from harmonics, kerf floor and walls as well as from tooth hops (Symes et al., 2010).

In forensic literature, characteristics useful for estimating TPI have not been extensively evaluated, despite this being an important feature to assist in distinguishing the different type of saws that perpetuators may use in criminal dismemberment cases (Bernardi et al., 2020).

Table 1: Saw mark characteristic definitions derived from Symes et al. (2010); Martlin & Rando (2020) and Nogueira et al. (2016).

Saw mark characteristic definitions	
False starts	A cut created by sharp tools that displays a floor, two walls, two floor corners and two initial corners.
Teeth per inch (TPI)	The measurement of the number of teeth found on the saw per inch.
Blade drift	The teeth mark of the saw that enters the bone material and creates a pattern on the kerf floor. Directional change of the blade can be derived and are more evident in false start lesions.
Bone islands	An island of bone material that remains in the kerf floor and displays a figure '8' pattern. Bone islands are created the same way as blade drifts where the saw enters the bone material and creates the pattern.
Breakaway spur	The terminal end of a bone section that exhibits a projection of uncut bone. This is created by the force that is applied during sawing and the breaking of the remaining bone tissue. The size is dependent on the force applied which sometime results in the fracture of the bone.
Exit chipping	Chipping (flaking) of bone at the end of a cutting stroke. Indicative of the sawing action and the point at which the blade exits the bone.
Harmonics	A side view expression of wave patterns that are three-dimensional (also known as peaks and valleys) in bone cross sections. Indicative of the direction of the blade as the saw progresses through the bone material.

Kerf	The floor and walls of a false start lesion. Kerf floors hold information on the distance between saw teeth (TPI) while kerf walls present information on the direction of the blade, amount of power and, as well as TPI. The width of the kerf can link to the thickness of the blade and the kerf length indicates the depth of the cut.
Pull-out striae	Scratches left by the saw which are withdrawn mid-stroke. Pull-out striae are perpendicular to the cut surface striations of the bone.
Striation regularity	Uniformity of the saw cut surface striations which may show directional changes of the saw blade. Uniform denotes consistently spaced parallel striations with no directional change, while non-uniform denotes non-parallel inconsistent spaced striations indicating directional change of the blade.
Tooth hop	Waves that appear in the cut surface striations caused by the blade movement on the bone. These usually occur in a straight pattern and the waves can be measured from peak to peak or dip to dip to calculate the distance of the teeth on the saw.
Profile shape	Kerf floor may be differently shaped, representing the type of saw that may have been used to create a lesion e.g., W-shaped indicates a crosscut saw and U-shaped indicates a rip saw.
Shape of the kerf wall	The blade contour as it cuts through the bone material creates a lesion shape of narrow and wide, straight or necking edges. These shapes are dependent on the teeth set of the blade used.

1.1.2 Methods for analysing saw mark trauma

Stereomicroscopy (SM) has traditionally been used to examine forensic tool marks; however, the advent of more powerful imaging technology has provided greater opportunity to examine characteristics not easily observed by eye. Thus, the need of a more powerful imaging tool, the scanning electron microscope (SEM) was introduced. Additionally, three-dimensional imaging can be produced by SEM which can be beneficial in analysing objects' surfaces (Freas, 2010; Thompson and Inglis, 2009).

Kooi & Fairgrieve (2013) used SM and SEM to analyse cut marks on burnt bones and found SEM useful for extracting cut mark length and depth, and to confirm results seen through SM. Saville, Hainsworth and Rutty (2007) established kerf marks by observing characteristics of

saw marks with support of SEM. In this way they were able to successfully observe and identify the saw marks caused by unique weapons in dismemberment cases.

Apart from using microscopy, the use of material to create casts of cut/saw marks has been shown to be effective in demonstrating tool mark characteristics in bones. To date, only limited research has been carried out on the methodology of casting material and how the application of the material to cut marks on bones is performed.

1.2 Heat-induced alterations to bone

1.2.1 Bone structure and composition

The bone matrix is made up of inorganic and organic components. The inorganic component is primarily calcium phosphate in the form of hydroxyapatite crystals. The organic component is primarily made up of Type 1 collagen. When fire comes into contact with the bone, the protein (organic) and minerals (inorganic) are significantly altered. This is a result of the bond between the components. The heat source at a specific temperature thus affects the components simultaneously but in different stages. The bone composition post-burning influences the structure which can be observed macro-microscopically (Castillo et al., 2013).

When observing trauma that is produced by heat, factors such as the skin, muscle and fat act as protective layers through which heat must travel before it reaches the bone (Pope & Smith, 2004). The heat exposure of bone is dependent on the different thickness and distribution of the soft tissue. Thermal destruction more readily affects parts of the bone that are thinner in soft tissue such as ulna and radius compared to the other parts of the body, making burn patterns more predictable (Pope & Smith, 2004). Bones exposed to fire present heat-induced change, and when examined both macroscopically and microscopically, changes to the colour, weight and size of the bones can be observed (Ellingham et al., 2015; Shipman, Foster & Schoeninger, 1984; Thompson, 2005; Vahirawongsakorn, 2022).

1.2.2 Heat-induced alteration to bone

The application of heat in the form of burning result in alteration to the structure and often gross morphology of bone. Such alteration includes colour change, fracturing, shrinkage, weight loss and deformation (Baby, 1954; Binford 1963; Carroll & Smith, 2018; Ellingham, Thompson & Islam, 2015; Herrman & Bennet, 1999; Koch & Lambert, 2017; Pope & Smith, 2004; Shipman, Foster & Schoeninger, 1984; Waltenberger & Schutkowski, 2017). The type

and level of alteration are influenced by a myriad of factors. Extrinsically these primarily relate to a combination of the temperature exposure and duration of burn (Ellingham et al., 2015; Symes et al., 2012). Intrinsically, this may be influenced by age, disease status, the presence of prior injury (size of surface area), and bone composition (Kimmerle & Baraybar, 2008; Symes et al., 2012; Waltenberger & Schutkowski, 2017).

During the process of burning, bone undergoes four stages of transformation: (1) bone dehydrates then goes through pyrolysis of organic compounds (decomposition). Thereafter, (2) loss of carbonates takes place which is inversion and, in the end, (3) the fusion of inorganic compounds and (4) crystal matrix coalescing occurs (Ellingham et al., 2015; Thompson, 2004; Waltenberger & Schutkowski, 2017).

The alteration process usually starts with dehydration between temperatures of 100-300°C. Thereafter, alterations to the primary structural characteristics in the mineralized bone tissue can be observed between temperatures of 300°C to 600°C. As the temperature increases from 600°C to 800°C contraction of the bone structure also increases. At these temperatures, the organic components are burnt completely. Crystals start to form and melt into one other, forming larger crystals at temperatures higher than 800°C. At the same time the bone structure is more fragile (Castillo et al., 2013).

When the bone is exposed to fire, a sequence of colour changes occur which might be able to denote the various stages of burning the bone has been through. In other words, it may be an indicator of thermal damage progression (Ellingham et al., 2015; Shipman, Foster & Schoeninger, 1984). As temperature and duration of burning increases bone will undergo colour changes associated with the loss of organic material as described above. Initially, bones exhibit a brown/yellow colour and eventually become black or carbonised. When the bones appear to have blue/white colour and are warped, fractured and distorted, the bones' organic material has been altered due to moisture being lost. Bones that are thermally altered in this manner are termed "calcined" (Ellingham et al., 2015).

Previous experimental studies have denoted slightly different colours for different stages of burnt bones. However, a general colour label can be distinguished as follows: at 200°C, a yellow-brown colour is seen, at 300-400°C, dark brown-black colour, at 500-600°C, ash-like grey colour and above 700°C, a chalky white colour is seen (Imaizumi, 2015). The colour provides information on how much oxygen was available and may infer what the fire temperature was. However, inference of burn temperature from bone colour should be

conducted conservatively due to the myriad of factors affecting colour change in bone (Ellingham et al., 2015).

Warping and shrinkage of bone is also observed during burning. Shrinkage of bone is noted at the temperatures between 700 ºC and 800 ºC (Thompson, 2004; Ubelaker, 2009). The rate of the shrinkage process continues to increases as the temperature increases while the weight reduction of the bone continuous to decrease, and at a certain point, ceases entirely. The decrease in bone weight occurs at temperatures of 400°C and may reach a plateau at approximately 700°C (Imaizumi, 2015).

Duration of the heat becomes an important factor as low temperatures might have minimal effect on bone shrinkage. However, when the duration is extended, provided that oxygen supply is sufficient, the bone will shrink. Liebenberg et al. (2023) compared dried and fresh pig femur (*S. Scrofa*) bones that were exposed to veldt (bush) fires of 5, 10, 20 minutes. The bones underwent shrinkage and measurements were significantly different between the two conditions of the bones. The authors found that dry bones shrunk up to 4.0% less after burning, while fresh bone also decreased in size up to 7.8%. Mineral composition and moisture of the bone may impact the degree of shrinkage in bone structure (Liebenberg et al., 2023; Moraitis & Spiliopoulou, 2006; Wieberg & Westcott, 2008).

A gradual reduction in bone volume can be observed around the temperature of 600°C, while a more rapid reduction occurs at about 1100°C, at which point bone volume has almost been halved (Imaizumi, 2015). In contrast, Thompson (2005) found that bones can increase in size subsequent to burning, therefore suggesting that heat-induced shrinkage should be considered carefully as this will affect accuracy of the analysis of burnt bones. The organic composition of the bone is burnt and leads to the contraction or expansion of bone structure (Thompson, 2004; Vegh & Rando, 2019; Waltenberger & Schutkowski, 2017).

The process of warpage and shrinkage also introduces fragmentation and heat-induced fracturing which typically occurs at temperatures above 500°C. The increase in cracks is proportionate to the elevation in temperatures; however, various studies have reported inconsistent temperatures at which fragmentation was observed. In some studies temperatures were low, falling between 100°C to 300°C, while in other studies fragmentation only occurred at temperatures above 1000°C (Imaizumi, 2015). Nonetheless, common fractures observed from burning include longitudinal, step, transverse, curved transverse, patina fractures,

delamination/splintering and heat line fractures (Herrman & Bennet, 1999; Symes et al., 2008) (Table 2).

Table 2: Definition of most common fracture types (Derived from Herrman & Bennet, 1999; Mata-Tutor et al., 2021a; and Symes et al., 2008).

Definition of fracture types	
Longitudinal fracture	The fracture is exhibited along the long axis of the bone and is the most common fracture found in burnt long bones.
Step fracture	Fractures that extend transversely from longitudinal fractures on the bone.
Transverse fracture	The fracture is perpendicular across the long axis of the bone, and may sometimes transect the bone. These fractures are common and are similar to step fractures.
Curved transverse fracture	Fractures that extend transversely from longitudinal fractures, but show an arc or oblique formation on the bone.
Patina fractures	Patina fractures appear in a uniform mesh of small cracks, and are typically found in the epiphyseal regions on the superficial layer of the bone.
Delamination & Splintering fractures	Delamination is the flaking of bone layers - separation of the cortical and cancellous bone, and occurs in the epiphyseal regions of the bone.
Heat line fracture	Heat line fractures are obvious indicators that separate the unburnt from the burnt surface of the bone.

Bones exposed to fires can be either fleshed or de-fleshed. In studies done by various authors (Baby, 1954; Binford, 1963; Thurman & Wilmore, 1980) de-fleshed bones exhibited longitudinal split fractures and some warping. In contrast, transverse fractures - where curvilinear patterns occur with irregular longitudinal split fractures – were observed in fleshed bones together with a greater degree of warping (Ubelaker, 2009). Thus, different types of fractures were observed, especially on the long bone diaphysis. When burnt bones display longitudinal splits, transverse cracks, reticular cracks, dendritic fissures, rough-surfaced

fracture and smooth-surfaced fracture, it may originate from pre-existing or inflicted trauma (Whyte, 2001).

In some cases, particularly in post-mortem burning, fractures on the bones caused by burning, need to be differentiated from those of a traumatic nature, for example saw marks (Kemp, 2016). The ability to differentiate between heat-induced and traumatic fractures is quite challenging, but still relatively achievable on a macroscopic level. However, resources on specific trauma characteristics that may remain after burning are limited (Scheirs, 2019).

1.3 Heat-induced alteration of pre-existing saw marks

The analysis of heat-induced alteration to pre-existing trauma and the ability to differentiate between traumatic fractures and heat-induced fractures has received considerable attention in recent years. This included studies investigating heat-induced alteration to blunt, ballistic and sharp trauma (including saw marks) (De Gruchy & Rogers, 2002; Herrman & Bennet, 1999; Koch & Lambert, 2017; Pope & Smith, 2004; Symes et al., 2012). Typical findings suggest extension, increased fragmentation and warping of pre-existing fractures. Various methodologies for burning have been applied, which may be broadly described as experiments using open, dynamic burning parameters (e.g., fire pits, natural fires) and experiments using closed, controlled burning parameters (e.g., furnace). The focus of this dissertation is on the alteration of saw mark characteristics (a form of sharp force trauma), thus, provided below is a review of relevant literature pertaining to this subject. A summary of these studies can be seen in Appendix A.

1.3.1 Open air experiments

Various researchers have conducted research on burnt bones to determine whether differences of pre-existing trauma before and after burning could be observed. The main intention of open-air experimentations is to construct sequential events leading up to death, and cases involve homicide, suicide, burnt human remains and fatal domestic fires. The primary focus of these studies is to distinguish peri-mortem and post-mortem trauma after recovering burnt skeletal remains (Carroll & Smith, 2018; De Gruchy & Rogers, 2002; Herrmann & Bennett, 199; Marciniak, 2009; Pope & Smith, 2004; Poppa et al., 2011).

When bones are analysed for tool marks, the structural integrity of the bones be compromised by heat exposure, causing the bones to fracture easily. This in turns leads to complication with

the individual and class characteristics of the bone when seeking to understand specifically when bones go through shrinkage as this will cause inaccurate assessment of kerf widths that were created by saws (Bailey et al., 2010). Ubelaker (2009) mentioned the challenges involved in differentiating heat-induced fractures and pre-existing fragmentation. However, studies that have been conducted indicate that pre-existing fractures can survive post-burning and therefore can be used to identify trauma marks pre-burning (Herrman & Bennet., 1999; Pope & Smith, 2004).

Sharp force trauma can be altered and morphed into multiple results due to external factors that influence the outcome. Examples of these factors include the presence of clothing or accelerants before or during burning, the amount of oxygen available, or even the environmental make-up (Ellingham et al., 2015; Marciniak, 2009). A study done by Mata-Tutor et al. (2022), investigated heat alterations on bones exposed to sharp force trauma post-burning. The authors found that the trauma marks were indeed disfigured, but still identifiable, despite fire exposure.

A study done by Marciniak (2009) compared the marks left by handsaws on bone to that of power saws, as well as the effect of burning on the saw marks created. False starts and complete cuts were created on semi-fleshed pig femur bones (*S. scrofa*) and it was found these marks were present in varying degrees (>400°C, ≥800°C) in the different burning stages. The bones were burnt in an open fire for a maximum duration of 3 hours, but were removed before structural destruction occurred. It was also found that the burnt bones retained saw marks from power saws and handsaws differently.

In similar burning conditions, Robbins, Fairgrieve & Oost (2014) performed a series of experiments analysing saw marks in pig bones created using 12 different kinds of saw blades. The cuts made were shallow and deep false starts. The maximum temperatures reached were between 710°C -720°C, which is slightly different from the study by Marciniak (2009). The results also showed that the false starts retained striations and were identifiable even in the calcined state of the bones. Saw mark characteristics, specifically tooth hops, were more prevalent after the bones were burnt.

Saw marks left by power saws were more difficult to identify due to variation in saw types, in which the number of striae produced by the blade differs. In contrast, handsaws rely on the sawing action of the individual, whereby the striae produced dependent on the manner in which the blade moves through the bones. However, it has been deduced that the overall saw mark

striae will still be identifiable after exposure to thermal heat (Marciniak, 2009; Robbins, Fairgrieve & Oost, 2014).

Kooi & Fairgrieve (2013) observed cut marks in fresh and burnt bone. The authors used semi-fleshed pig ribs (*S. scrofa*) as proxy for human bones. Knife and stab wounds were created by two newly purchased knives (smooth and serrated edged). The ribs were then burnt in an open fire pit for approximately 1 hour or until minimal tissue was seen. The bones appeared to be calcined to a varied degree, and heat-induced (longitudinal and transverse) fractures were present. The prevalence of the cut mark characteristics was less in burnt bones than in fresh bones overall. The appearance of cut marks in burnt bones were affected by the fire along with heat-induced fractures and residual tissue. In addition, striae from the cut marks were not clearly observable in fresh or burnt bones.

Poppa and colleagues (2011) carried out a study utilising fleshed pig heads. Lesions made by sharp force tools including the saw were created and burnt on an iron grill using gas cookers. The saw marks were broken and affected by fractures, but a linear shape and irregular edges were recognisable. The authors stated that morphological characteristics lose distinctiveness during carbonisation but became more visible towards the calcined stage due to soft tissue the being burnt. Nevertheless, the irregular edges caused by the friction from the saw and bone were identified with the aid of a microscope, could be distinguished from fractures.

An interesting experiment by Koch & Lambert (2017) analysed how the duration of fires would impact pre-existing trauma. Two separate burns were carried out, in which the one burn duration was 8 minutes at approximately 800°C and the other was 22.5 minutes at approximately 1000°C. The fire was started in a built compartment made of cement boards to simulate an indoor setting. Pig carcasses (*S. scrofa*) were subjected to various types of traumas, but sharp force trauma will be reviewed for the purpose this study topic. A knife was used to create the trauma on two carcasses, and each carcass was burnt in the separate fires. Trauma was detectable both pre- and post-burning in the first burn experiment, while in the second burn experiment, trauma on the burnt carcass was less detectable than prior to burning.

1.3.2 Furnace experiments

Some of the earliest experiments recreating fire conditions in order to analyse the gross changes of bone are done by authors Baby (1954); Binford (1963); and Shipman, Foster & Schoeninger (1984). Thus, laboratory studies have gradually increased over the years, whereby bones are burnt in kilns, ovens or furnaces (electric or gas). Temperatures can be selected at set intervals

to observe heat-induced alterations on bones (Carroll & Smith, 2018; Collini et al., 2015; Ellingham, Thompson & Islam, 2015; Shipman, Foster & Schoeninger, 1984). Therefore, burning temperatures, duration of burning, trauma types as well as the type of bones used, vary across studies. Although, laboratory settings do not mimic the reality of an open-fire setting, these experiments allow for greater control of variables to be explored.

An experiment carried out by De Gruchy & Rogers (2002) utilised pig forelimbs through which a cleaver and a knife were used to create chop marks on bone. After the bones were burnt, heat-induced fractures were identified, but it was noted that trauma inflicted on the bones by the cleaver were more inclined to fragmentation than chop marks. However, sharp force trauma was able to survive the burning process.

On the other hand, Macoveciuc et al. (2017), aimed to solve any dissimilarities between controlled and field experiments. The methodology carried out in the study was to analyse the types of heat fractures and whether it is related to mechanical trauma that exists before heat exposure. Juvenile sheep radii were subjected to sharp trauma, through which cut marks were inflicted by a knife. The knife was attached to a rig and dropped onto the long axis of the bone perpendicularly. The bones were burned in an electric furnace with the maximum temperature of 820°C with a heat exposure duration of four hours. It was found that sharp trauma was enhanced with thermal fractures present (Macoveciuc et al. 2017). The authors deduced that it was possible to trace the origin of the initial trauma pre-burning from heat-related fractures.

A similar methodology by Waltenberger & Schutkowski (2017) made use of kitchen knives to penetrate the skin and the rib surface through a guillotine gadget that would simulate the stabbing action. While Waltenberger & Schutkowski (2017) used juvenile pig ribs (*S. scrofa*) covered with soft tissue, the ribs were burnt in an electric furnace with a duration of three hours at 700°C. Once the ribs were cooled in the furnace, the authors identified longitudinal heat-induced fractures with the cut marks. Furthermore, literature suggests that bone shrinkage alters cut marks; however, in this case the authors found that the cut marks were unaffected.

Similarly, Vachirawongsakorn, Painter & Márquez-Grant (2022) found that cut marks were still identifiable post-burning; however, it was also discovered that morphological/dimensional changes to the trauma created could take place, especially at higher temperatures around 800°C. The authors compared kerf dimensions and morphology inflicted on pig rib bones (*S. scrofa*) by kitchen knives, pre- and post-burning. The bones were burned in an electric furnace at 850°C for 30 minutes and were allowed to cool down to room temperature. Apart from burn duration,

bone age may also alter the cut marks dimensions, especially after the bones are exposed to heat. (Vachirawongsakorn, Painter & Márquez-Grant, 2022).

Furthermore, the study distinguished that heat-induced fracture can be differentiated from skeletal traumatic lesions. This study observed that the cut marks were identifiable by the linearity in which features were narrow with raised or smooth margins. This contrasted with heat-induced fractures which displayed random crack formation with clear-cut borders.

Vegh & Rando (2019) stated that kerf widths that underwent 1000°C burn degree changed metrically, which is in agreement with Vachirawongsakorn, Painter & Márquez-Grant (2022), but contrasts the statement by Symes et al. (2012) that no changes in metrics for pre- and post-burning bones occurred. The trauma wounds were inflicted by a knife and a hacksaw on de-fleshed porcine (*S. scrofa*) long bones. Vegh & Rando (2019) showed that 20 minutes at 1000°C could change the kerf widths. The Symes et al. (2012) experiment showed that temperatures may not have been high enough, with sufficient exposure time, to change the kerf widths.

Mata-Tutor et al. (2021b) conducted research analysing the sharp force trauma in dismemberment scenarios using burnt cadavers. A kitchen knife was used to create cut marks while a machete was used to create chopping marks. The authors found that 7 out of the 55 injuries inflicted by sharp tools survived post-burning, while heat-induced fractures were also identified. Even so, several variables could have influenced the results. It should be noted that the cadavers were exhumed from the cemetery and were embalmed. Also, the oxygen availability and temperature in a crematorium furnace differs greatly to that of an open pyre (Liebenberg et al. 2023). Nevertheless, this research can still contribute valuable information to forensics, as there are many cases presenting extensive variation in both humans and taphonomic conditions.

The effects of heat alteration on pre-existing sharp force trauma on bones can be significant and may impact the accuracy of forensic analyses. The above-mentioned studies highlight the need for careful analysis and interpretation of trauma on heat altered bones. A better understanding of the mechanisms of heat alteration on bone tissue is required, and a more effective method should be developed for future references.

1.4 Conclusion

While extensive research has been conducted on characteristics associated with saw marks (Marciniak, 2009; Nogueira et al., 2016 & 2018; Robbins, Fairgrieve & Oost, 2014; Symes et al., 1992, 2010), this research has not necessarily expanded to determine the ability to detect such characteristics post-burning. The provided review indicates heat-induced alteration to sharp force trauma has been investigated. However, few studies have investigated alterations to saw mark characteristics. Such studies are necessary because it is important to establish whether it is possible to differentiate between the effect of heat-induced or inflicted trauma, as the results may contribute towards the criminal investigations and the forensic science fields.

Most of the previous research has been conducted outdoors (Kooi & Fairgrieve, 2013; Marciniak, 2009; Mata-Tutor et al., 2022; Pope & Smith, 2004; Poppa et al., 2011; Robbins, Fairgrieve & Oost, 2014; Waltenberger & Schutkowski, 2017), and although this mimics reality in forensic context with fluctuating temperatures, systematic research is needed at controlled temperatures to fully understand the impact of heat on bones. This would provide information on the specific temperatures at which heat-induced alterations occur.

Furthermore, while research has investigated morphological changes, limited analysis of metric changes has been conducted. Literature provides most information on bone deformation, but rarely informs on how much the bones might have shrunk or expanded, not to mention on saw mark characteristics.

Moreover, the majority of animal models used have been domestic pig bones, citing similarities in bone compositions to humans. However, the size and shape of porcine bones (which may affect bone biomechanics) is markedly different from human bone. As such further research on animal models is needed. Additionally, the condition of the animal bone, particularly dry bones, for experimentation has been questioned. Dry, fresh and fleshed bones would differ significantly in research development as suggested by Liebenberg et al. (2023); Nogueira et al. (2018); Norman et al. (2018b); and Pope & Smith, 2004. Information regarding this can contribute to the knowledge of this topic and allow for improvements to be made in future research.

Experiments in burnt bone analysis has grown over the years, and studies such as these, contribute to the improvement and further advancement of predictions surrounding burn temperatures and the resultant heat effects on bones. Nonetheless, there are techniques that still

need refinement and deeper understanding of additional factors that could influence this type of research is necessary.

Aim of Study

The aim of the study is to assess and compare morphometric and morphologic saw mark characteristics inflicted on non-human bone and subsequently assess changes in trauma characteristics following burning at various controlled temperatures. This will be achieved by inflicting trauma to the mid-shaft of sheep femur bones using a saw. The trauma will then be analysed, measured and compared. The bone specimens will be subjected to various degrees of heat through the use of a muffle furnace and reanalysed to determine any differences.

Hypotheses

1. The temperature at which bones are burnt will indicate the extent of fracture pattern and discolouration.
2. The higher the burn temperature, the more thermal alteration on saw mark characteristics will occur.

CHAPTER 2: Materials and Methods

2.1 Specimens

Eighteen whole lamb (*Ovis aries*) femur bones (N=18), sourced from various butcheries in Cape Town, South Africa were utilised in this study. Sheep bones were selected as they are similar in shape and structure to human femurs. Furthermore, these bones have previously been utilised as proxies to human bones in the evaluation of fracture mechanics (Dempsey et al., 2019; Reber & Simmons, 2015) and in the evaluation of burning (Macoveciuc et al., 2017; Thompson, 2005).

The bone specimens were stored in a freezer (-20°C) until experiments and testing were conducted. Soft tissue found on the bones was removed by means of manual dissection leaving the periosteum intact. Prior to conducting the experiments and testing procedures, the specimens were thawed at room temperature for approximately 24 hours. Torimitsu et al. (2014) has demonstrated that freezing of bone at -20°C for the period of three months with subsequent thawing, has little effect on the mechanical properties of bone.

Saw marks were inflicted onto each bone which was subsequently evenly divided into three experimental groups to be burned at 400°C, 600°C and 800°C burn temperatures. To ensure consistency of specimens between burn groups, a prior biomechanical analysis was completed on each bone. This included measuring the length and width of the bone shafts followed by the calculation of the bending moment in bones. Bones were divided into each test group ensuring no significant difference in biochemical structure of specimens between groups (Appendix B). The total weight of each bone specimens was recorded using a laboratory scale before and after incinerating the specimens (Appendix E).

2.2 Saw mark trauma

The 18 specimens were subjected to sawing action with a backsaw/tenon saw to the anterior mid-diaphysial region. A backsaw/tenon saw (alternating tooth set) with 13 tooth per inch (TPI) was newly purchased for the purpose of this research (Figure 1). This saw was chosen as it is one of the most common tools used for sawing and is readily accessible.

Figure 1: 13 TPI backsaw used in the study.

Each bone was placed on a mitre block that was securely attached to the laboratory bench by two G-clamps (Figure 2). Three types of cut marks were made on the mid-shaft of each bone specimen which included: a shallow false start, incomplete cut/deep false start and a complete transection of the bone (Figure 3). Each of the three cuts was created by the same blade and by push and pull motions of the saw perpendicular to the long axis of the bone. The saw was handled by the same person to maintain the same force and regularity in addition to the angle and consistency. Thus, a total of 72 cut surfaces were analysed from 54 cuts/lesions. Lesions were photographically recorded and assessed by means of casting.

Figure 2: Mitre block secured with G-clamps.

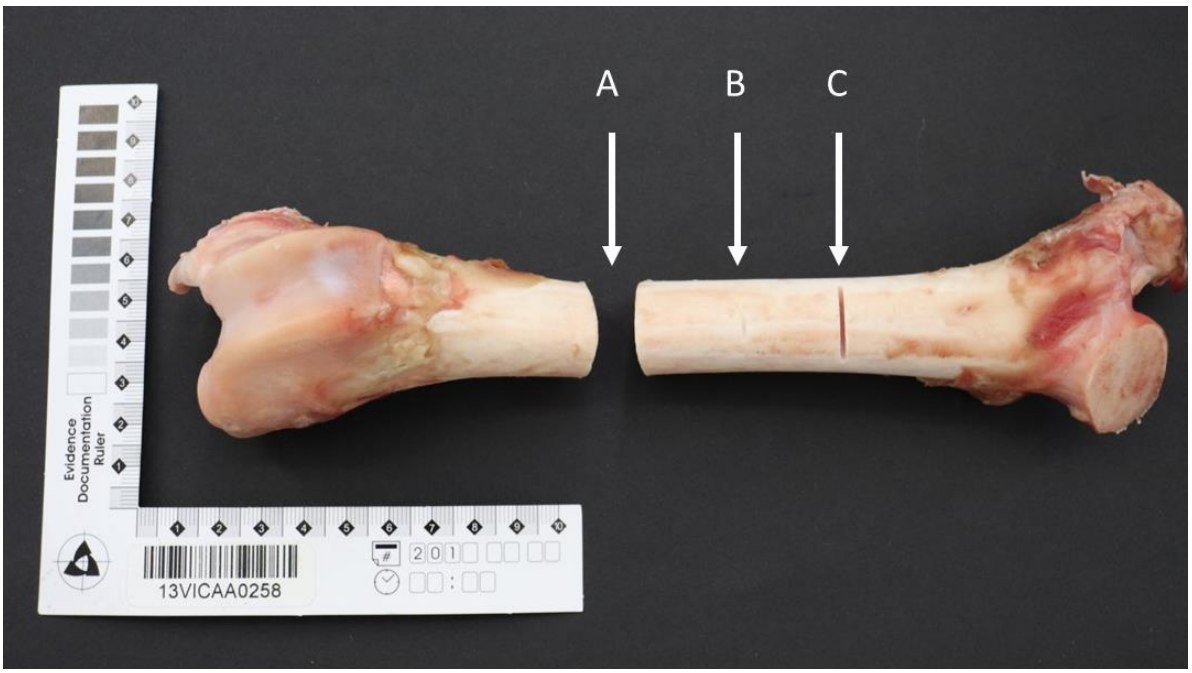

Figure 3: Different cut types inflicted onto the mid-shaft of femur bone. A) Complete transection, B) Shallow false start lesions and C) Incomplete cut/deep false start.

2.3 Burning

After the de-fleshed lamb bones were subjected to saw mark trauma, the specimens were burned in a muffle furnace (Labofurn, Kiln Contracts Pty Ltd., Cape Town, South Africa) at three different controlled temperatures (400°C, 600°C and 800°C). Bones were individually placed into the muffle furnace on a heat proof ceramic tray at the desired temperature and allowed to burn for 20 minutes. After burning, the bones were removed and left to cool overnight. While the use of an electric furnace may not mimic real life burning events, the furnace allows for the analysis at controlled temperatures and duration, which is not possible in an open fire environment. This allows for more accurate inference of the role of temperature in a burning event (Ellingham et al., 2015; Shipman, Foster & Schoeninger, 1984). Once the specimens had cooled down, the saw marks were compared, measured and photographically recorded. Non-metric alterations to trauma and fracture surface characteristics were visually assessed. The results of the burnt bones were compared to the results collected prior to burning – to assess alteration of saw mark characteristics.

2.4 Saw mark characteristics

Saw mark characteristics (Symes, 1992; Symes et al., 2010) were recorded before and after burning to assess any changes in trauma morphology. Fractures, kerf depths and widths, saw

striations, and break away spurs were measured and photographically recorded. The presence/absence of exit chipping, blade drift, bone islands, pull-out striae and tooth hop were also recorded. The profile of false start cuts and the shape of the kerf floor were classified according to the morphology of the cut.

The assessment of these traits was conducted macroscopically as well as through a stereomicroscope, and the results were recorded both in a Microsoft® Excel spreadsheet and photographically. Certain characteristics, especially profile shape and kerf depth of false starts and incomplete/deep false cuts, were analysed and measured from casts. Each cut type was analysed as shown in Table 3. Casting materials (Platinum silicone by Amt. composites, (Appendix F1)) were purchased from local suppliers in Cape Town, South Africa. Black fingerprint powder was applied onto unburnt bones to visually enhance the characteristics (Appendix F2). A camera (Canon EOS 650D/800D) was utilised to photograph the specimens with a scale. A digital calliper as well as a software program ImageJ Version 1.53k (2021, USA: National Institute of Health) were utilised to measure the various saw mark characteristics.

The unburnt and burned bones were observed under the stereomicroscope (Zeiss Discovery V20) and the characteristics were determined to be present or absent. The characteristics are listed (Table 3) and recorded according to the different cut types separately and where the trait is applicable in the specific cut type. Photographs of each cut type were taken through the stereomicroscope for the prevalence and assessment of the characteristics. Characteristics such as the profile shapes, the depth of false starts and incomplete cuts (deeper false cuts) were analysed from casts under the stereomicroscope.

Table 3: Criteria for the analysis of various cut types for pre- and post-incineration of bone specimens.

Cut type	Characteristic	Variable type	Description
False Starts and incomplete cuts	Maximum kerf width	Numerical	Measured between the two edges of the kerf walls on each of the bones.
	Maximum average kerf depth	Numerical	Measured on the casts of each cut/lesion.
	Blade drift	Categorical	Assessed the pattern of the walls.
	Bone islands	Categorical	Assessed the midline of the kerf floor.
	Profile Shape	Categorical	Assessed the casts of each cut/lesion.
	Shape of the floor	Categorical	Assessed the cut edges and floors to determine whether it was straight, narrow and wide or necking.
	Exit chipping	Categorical	Presence or absence of chipping especially found in incomplete cuts and complete transections assessed on the superficial part of bones.
Complete transections	Breakaway spurs	Numerical & Categorical	Maximum length and thickness of the spur measured. Presence or absence of the spur was assessed at the terminal end of the cut.
	Harmonics	Categorical	Presence or absence assessed on the side view of the cut.
	Pull-out striae	Categorical & Numerical	Presence or absence of the perpendicular striae assessed. If present on the cut surface, the number of striations was recorded, and the average distance was measured.
	Tooth hop	Categorical	Presence or absence on the cut surface and the number of tooth hops was recorded.
	Striations	Numerical & Categorical	The average distance was measured on the cut surface and recorded. Assessed linear ridges on cut surface whether uniform or non-uniform. The consistency of the cut was assessed and recorded as either uniform or non-uniform.

2.5 Data Analysis

The data collected was statistically analysed using IBM SPSS Statistics for Windows, Version 28.0 (2021, Armonk, NY: IBM Corp) software. All the variables were recorded before and after incineration and the data distribution was tested for normality using the Shapiro-Wilk test for numerical data only. To compare the recorded data before and after burning for the degree of the variable's relationship, the paired *t*-test was applied. The Wilcoxon signed rank test was

carried out for data that was not normally distributed. All statistical tests were conducted at a significance level of $\propto = 0.05$.

2.5.1 Inter/intra-observer error

Inter/intra-observer error was also performed in a random subset containing 50% of the total sample. Both unburnt and burnt samples were analysed by the author and an observer to ensure consistency and repeatability of results. Inter/intra-observer error was reported as a percentage concordance for categorical variables and intraclass correlation values calculated for numerical variables.

2.6 Ethical clearance

Ethical clearance was obtained from the Animal Ethics Committee (AEC) of the University of Cape Town (UCT) prior to commencement of the research (AEC reference number: 022_015) (Appendix C). The bone specimens procured from the local butcheries were prepared according to the butcheries' guidelines and rules. The animals were not slaughtered for the purpose of this experiment but rather for the purpose of human consumption.

CHAPTER 3: Results

3.1 Observer error results

3.1.1 Inter-observer

All categorical variables observed between the observers were found to be 100% congruent, except for the interpretations on the presence and number of tooth hops in unburnt bones which had a percentage concordance of 77.8% and 83.3% for burnt bones. The analysis of tooth hops macroscopically and microscopically was challenging; nonetheless, this characteristic was still identifiable for the backsaw used in this research.

The intraclass correlation for the numerical variables between the observers indicated excellent and moderate reliability and are significant (Table 4). The average distance between the striation were difficult to observe as the location on the cut surface was diverse leading to dissimilar results. Therefore, the intraclass correlation value for the characteristic could not be calculated.

Table 4: Intraclass correlation results of numerical variables for inter-observer.

Characteristic	Mean difference (mm)	ICC-value	P-value
Average kerf width (unburnt)	0	0.616	0.003
Average kerf width (burnt)	0.37	0.958	< 0.001
Average kerf depth (unburnt)	0.442	0.998	< 0.001
Average kerf depth (burnt)	0.784	0.999	< 0.001
Breakaway spur thickness (burnt)	1.690	0.643	0.003
Breakaway spur length (burnt)	2.910	0.744	< 0.001

3.1.2 Intra-observer

The intra-observer results for categorical variables were found to be slightly different especially in pull-out striae with percentage concordance of 88.9% and 83.3% for unburnt and burnt bones respectively. Tooth hops had percentages concordance of 83.3% for unburnt bones while the burnt bones were 94.4%. While the rest of the variables were 100% congruent.

The intraclass correlation values of the numerical variables for the intra-observer shown moderate to excellent reliability. However, a few values were poor especially for the average distance in striation marks (Table 5). This could be due to the random location points selected

on the cut surface for measurement. Nonetheless, the results were still significant. The burnt bones were relatively easier to observe and measure compared to the unburnt bones.

Table 5: Intraclass correlation results of numerical results for intra-observer.

Characteristic	Mean difference (mm)	ICC-value	P-value
Average kerf width (unburnt)	0.220	0.829	< 0.001
Average kerf width (burnt)	0.550	0.941	< 0.001
Average kerf depth (unburnt)	0.488	0.998	< 0.001
Average kerf depth (burnt)	6.964	0.949	< 0.001
Striation distance (unburnt)	0.260	0.171	0.150
Striation distance (burnt)	0.111	0.525	0.004
Breakaway spur thickness (burnt)	2.090	0.593	0.004
Breakaway spur length (burnt)	0.790	0.929	< 0.001

3.2 Discolouration, fragmentation/fractures and weight

A visual assessment of the bones post-burning revealed that bones exposed to varied controlled temperatures, displayed various levels of discolouration (Appendix D). Bones exposed to a 400°C controlled temperature emerged mostly carbonised showing a tinge of brown colour. In this group, the specimens were charred and had a greasy bone appearance. In the 600°C burn temperature group, a grey/black as well as a grey/blue colour was observed on the bones. Bones in the 800°C group appeared to be milky-white and grey-white colour with grey-blue patches. The specimens became more fragile as the temperature increased, and in the highest temperature group, bones had a delaminated (chalky-like) appearance which could represent the beginning stages of bone calcination; however, all the bones were carbonised (Figure 4).

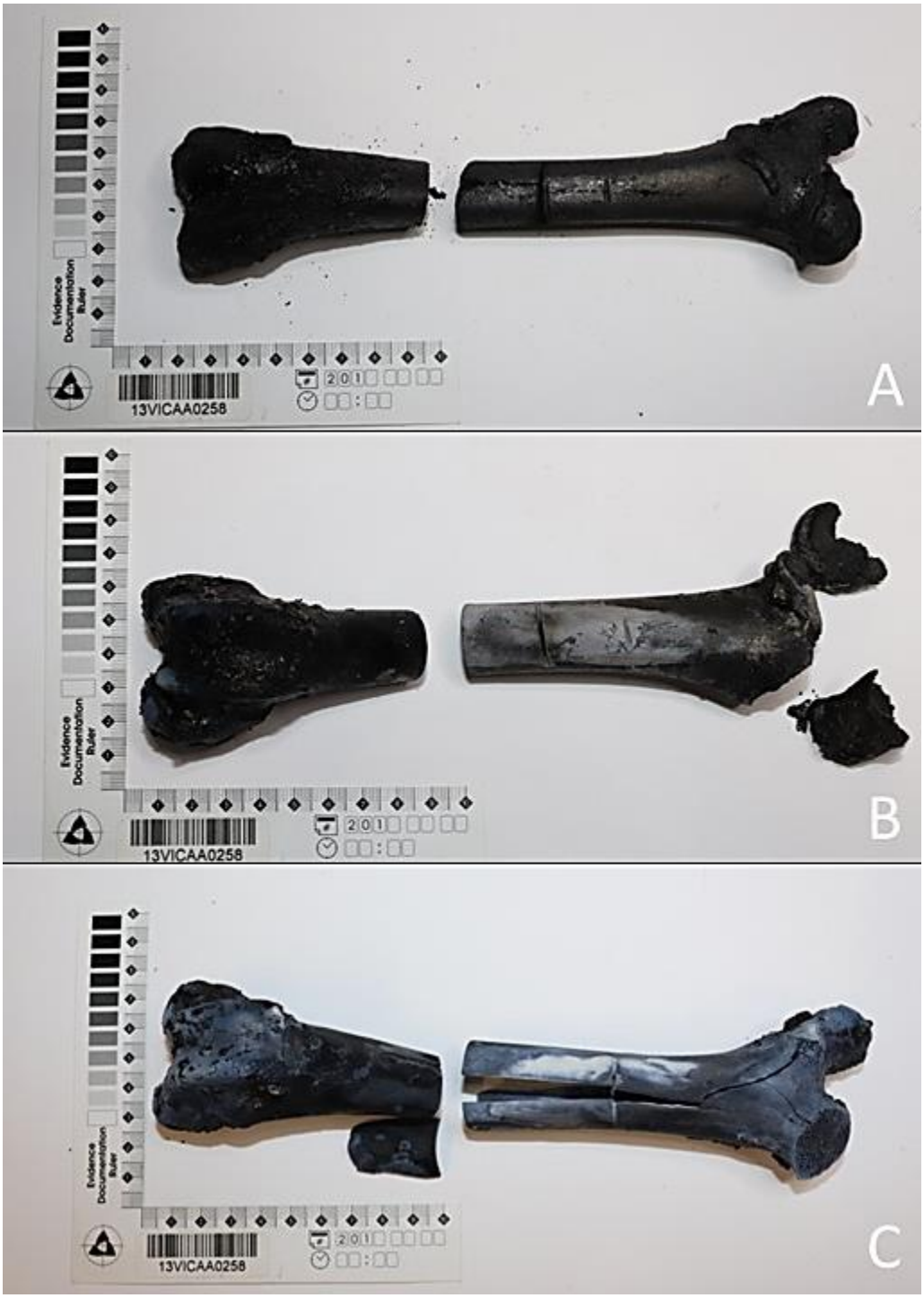

Figure 4: Bones burnt at various controlled degrees. A) 400°C, B) 600°C and C) 800°C.

Heat-induced fractures can be classified into transverse, curved transverse, longitudinal, delamination and splintering, and patina (Binford, 1963; Herrman & Bennet., 1999; Shipman, Foster & Schoeninger, 1984; Symes et al., 2008). These fractures are defined by the direction through which the fracture propagates and the location where it occurs. As expected, heat-induced fractures were frequently observed in all the bone samples.

Crack formation occurred in all the bone specimens leading to fragmentation. Heat-induced fractures occurred across the bone shaft in both longitudinal and transverse planes including fractures that appeared to originate from the inflicted marks. The different saw cut marks were easily distinguishable from heat-induced fractures due to the uniformity and rougher edges associated with the saw marks (Figure 5). However, identifying the heat-induced fractures was more challenging when bones were burnt at the high burn temperature (800°C).

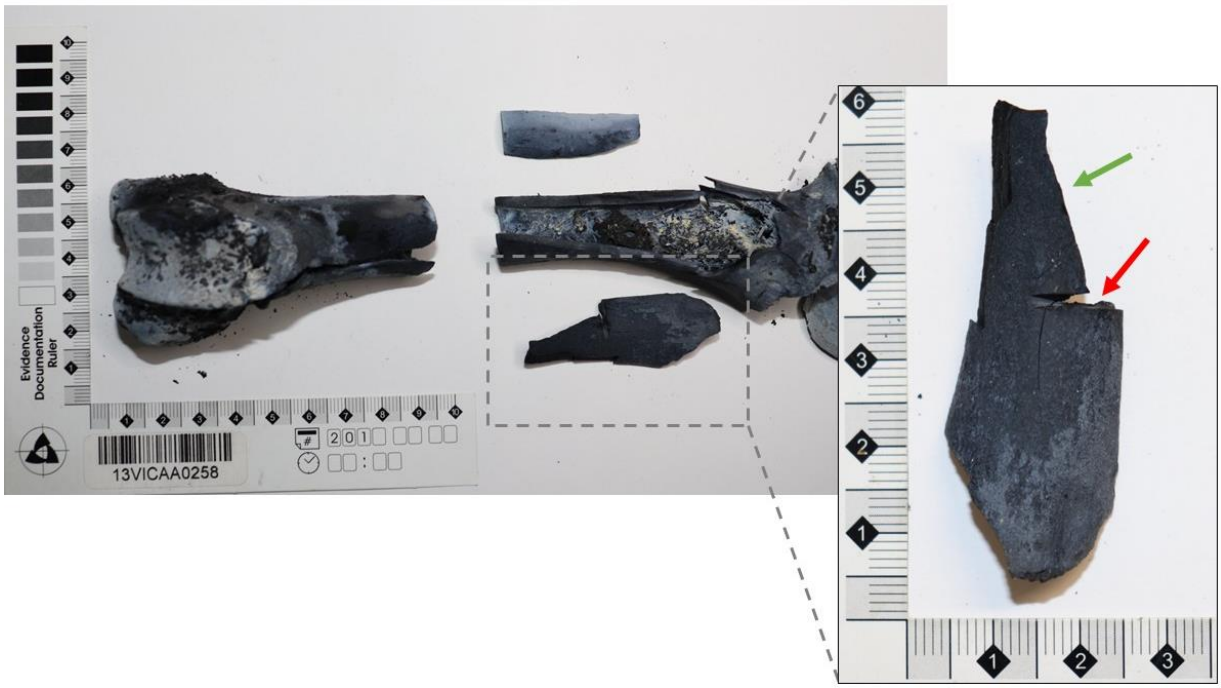

Figure 5: Heat-induced fracture (green arrow) originating from the incomplete cut (at 800°C) and can be differentiated from saw mark (red arrow).

In the 400°C burn group, longitudinal fractures totalled to 19, and compared to the 600°C and 800°C, this fracture type occurred 18 and 43 times respectively. Step fractures were less common than longitudinal fractures, nonetheless two step fractures appeared in the 400°C group, while three and 15 in the 600°C and 800°C groups. Similarly, to step fractures, transverse fractures appeared thrice in 400°C group, 600°C had five and 800°C had 16 fractures. Curved fractures appeared had a moderate amount where five, nine and 19 fractures appeared in 400°C, 600°C, 800°C respectively. Patina fractures ranged from none to moderate while delamination and splintering fractures ranged from minimal to multiple instances across all temperatures (Table 6) (Appendix D).

The longitudinal fractures were visibly split perpendicularly to the false start lesions and incomplete cuts, transverse fractures originated from the incomplete cuts. Heat-line fractures

were not observed as the heat exposure to the bones was distributed quite evenly in the furnace. Most heat-induced fractures were identified in the 800°C burn group. The weight of the bones decreased after burning (Appendix E) resulting in shrinkage in all the bones; in addition, warping was evident in the 800°C burn group.

Table 6: Fracture types in different temperature groups.

Heat-induced fractures	**Temperature groups**			**Total heat-induced fractures**
	400°C	**600°C**	**800°C**	
Longitudinal	19	18	43	80
Step	2	3	15	20
Transverse	3	5	16	24
Curved transverse	5	9	19	33
Patina*	None	Minimal	Minimal - Moderate	None – Moderate
Delamination & Splintering*	Minimal-Moderate	Minimal - Moderate	Moderate - Multiple	Minimal – Multiple
Heat line fracture	None	None	None	None

*Note: None-absent; Minimal-average amount; Multiple-Numerous amounts.

3.3 False start lesions

3.3.1 Kerf width & kerf depth

Overall, the mean kerf width (Figure 6) in unburnt bones was 1.022 mm (SD=0.220 mm). Following burning there was no significant difference between the kerf width in unburnt bones compared to bones burnt ($\bar{x}$=1.233 mm; SD=0.159 mm) at 400°C (p=0.82). At 600°C the mean kerf width of the burnt bones was 1.187 mm (SD=0.166 mm) which is significantly greater (p=0.010) than the unburnt bones ($\bar{x}$=0.883 mm; SD=0.202 mm). At 800°C there was yet again no significant difference (p=0.403) in the mean kerf width between the burnt bones ($\bar{x}$=1.100 mm; SD=0.282 mm) and the unburnt bones (1.21 mm; SD=0.075 mm) (Figure 7).

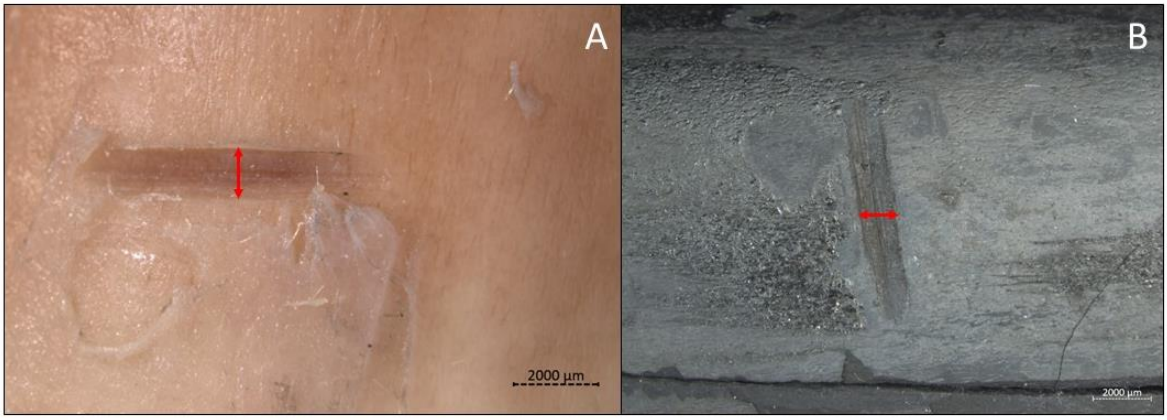

Figure 6: The kerf width of false start in A) unburnt and B) burnt bone.

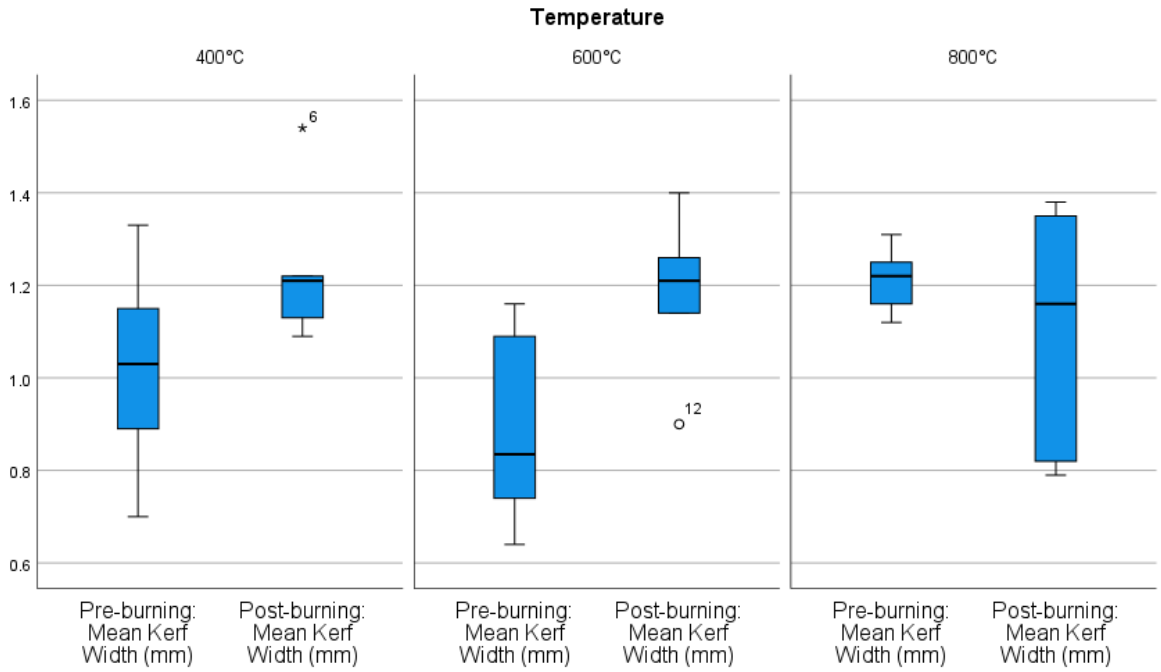

Figure 7: Box plots of false starts mean kerf widths (millimetres) before and after burning in each burn temperature group.

The mean kerf depth of the burnt bones ($\bar{x}$=0.792 mm; SD=0.084 mm) at 400°C was not significantly different (p=0.578) from the unburnt bones ($\bar{x}$=0.842 mm; SD=0.241 mm). The bones burnt at 600°C with mean kerf depth of 0.695 mm (SD=0.155 mm) was also not significantly different (p=0.682) than the unburnt bones with mean kerf depth of 0.732 mm (SD=0.087 mm). However, the mean result of unburnt bones is 0.788 mm (SD=0.059 mm) at 800°C. In burnt bones, only one of the six false starts were recovered, with a mean kerf depth

0.504. Consequently, the standard deviation of burnt bones and the significance cannot not be calculated (Figure 8).

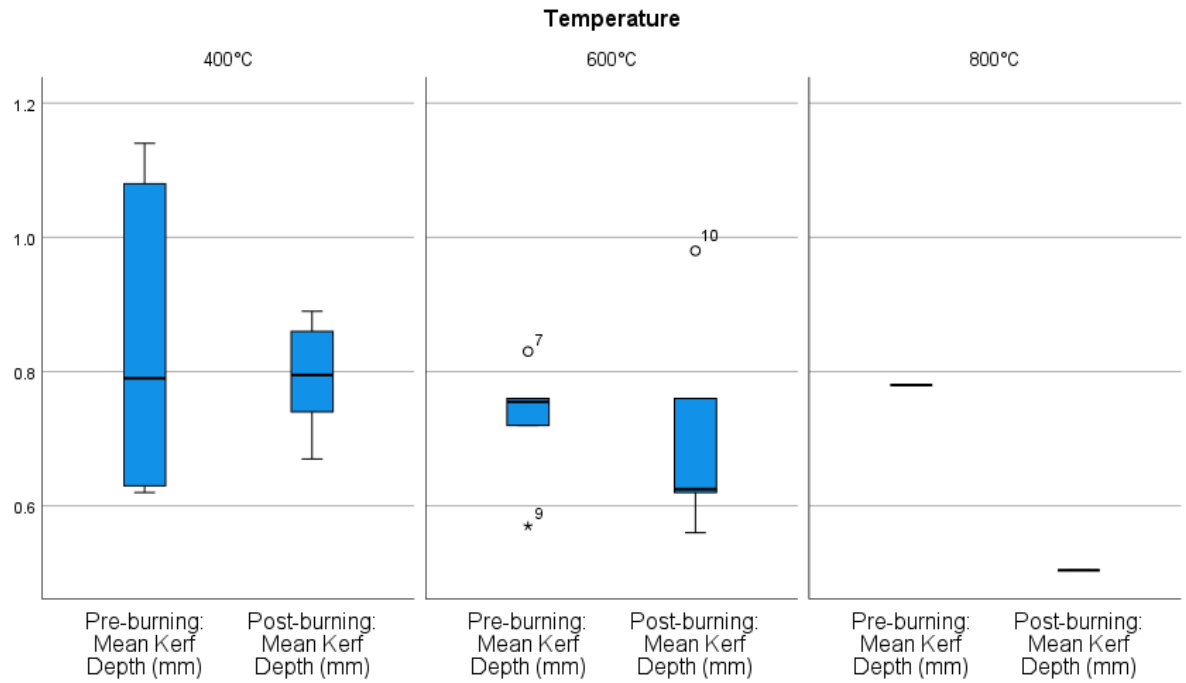

Figure 8: Box plots of false start kerf depths (millimetres) before and after burning in each burn temperature group. Only one false start could be recovered in the 800°C burn group; thus, no accurate results are shown.

3.3.2 Blade drift & bone islands

Neither blade drift nor bone islands were observed in false starts before and after burning the specimens at 400°C, 600°C and 800°C (Table 7).

3.3.3 Profile shapes

The profile shape of 18 unburnt bones were predominantly round shaped present in 17/18 (94.4%) bones while 1/18 (5.6%) was square with round corner shaped. After burning, 11/18 (61.1%) were round shaped, and 2/18 (11.1%) square with round corner shaped (Figure 9). In burnt false start lesions, 5/18 (27%) of profiles could not be recovered.

All six of the unburnt specimens showed round shapes and after burning the bones at 400°C, five out of the six bones were round shaped. The one other bone was classified to have a round shape pre-burning; however post-burning resulted in square with round corner shaped (Table 7).

In the 600°C temperature group, five out of six unburnt bones were observed to be round shaped, and one were found to be square with round corners. After burning, the number of profile shapes were the same; however, four samples remained the same being round shaped, while two bones changed after burning. The one bone was round shaped prior to burning, but identified to be square with round corner shaped after burning, and vice versa for the other bone.

Round shaped profiles were observed in all six unburnt bones; however, after burning the bones at 800°C, only one round shaped profile could be identified. The false starts after burning were mostly too fragile to recover and collect any data.

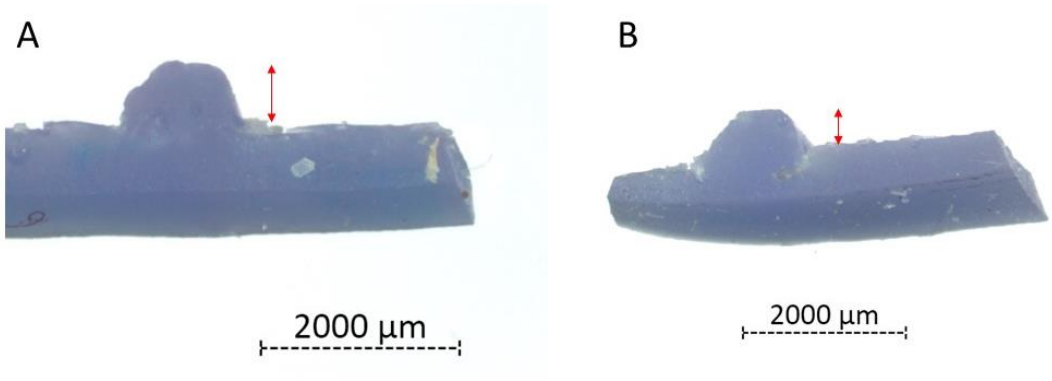

Figure 9: Profile shapes of false starts. A) Round shape and B) square with round corner shape.

Table 7: Mean measurement and presence of saw characteristics of false start lesions.

Characteristic	400°C		600°C		800°C		Total cuts analysed
N=18	**Pre-burning**	**Post-burning**	**Pre-burning**	**Post-burning**	**Pre-burning**	**Post-burning**	**Per Temperature group**
Mean Kerf width (mm)	1.022 mm	1.233 mm	0.883 mm	1.187[a] mm	1.25 mm	0.917 mm	6
Kerf depth (mm)	0.842 mm	0.792 mm	0.732 mm	0.695 mm	0.787 mm	0.504[a] mm	6
Blade drift	0 (0%)	0 (0%)	0 (0%)	0 (0%)	0 (0%)	0 (0%)	6
Bone island	0 (0%)	0 (0%)	0 (0%)	0 (0%)	0 (0%)	0 (0%)	6
Profile shape	6 Round-shapes	5 Round-shapes 1 Square with round corners	5 Round-shapes 1 Square with round corners	5 Round-shapes 1 Square with round corners	6 Round-shapes	1 Round-shape 5 – N/A (could not be collected)	6
Shape of the wall	Straight	Straight	Straight	Straight	Straight	Straight	6

[a]shows statistical significance ($p < 0.05$) between pre-burning and post-burning in kerf width and kerf depth.

3.4 Incomplete cuts/lesions

3.4.1 Kerf width & kerf depth

The incomplete cuts were also compared before and after burning. The mean kerf width for the unburnt and burnt bones at 400°C were 1.154 mm (SD=0.009 mm) and 1.194 mm (SD=0.145) respectively (Figure 10). There was no significant difference before and after burning (p=0.588). One measurement post-burning could not be collected due to the bone splitting in two at the cut. At 600°C there was also no significant difference (p=0.963) in the mean kerf width between burnt ($\bar{x}$=1.150 mm; SD=0.061 mm) and unburnt bones ($\bar{x}$=1.148 mm; SD=0.040 mm). For 800°C, the mean kerf width was 1.353 mm (SD=0.857 mm) for burnt bones which is significantly greater (p=0.001) than the unburnt bones with 1.182 mm (SD=0.331 mm) (Table 8).

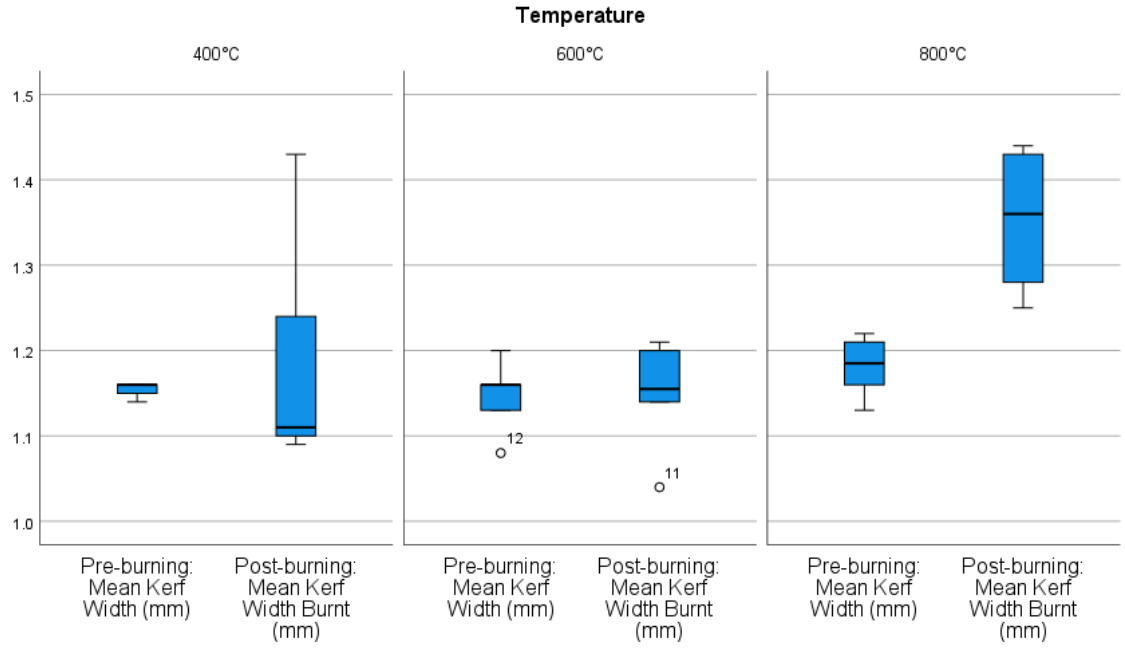

Figure 10: Box plots of incomplete cut mean kerf widths (millimetres) before and after burning in each burn temperature group.

No notable difference (p=0.783) arose between kerf depth (Figure 11) for unburnt ($\bar{x}$=5.305 mm; SD=2.009) and kerf depth burnt bones ($\bar{x}$=5.400 mm; SD=1.576 mm) at 400°C. Similarly, at 600°C there was no significant difference (p=0.713) in the mean kerf depth between the burnt bones ($\bar{x}$=5.048 mm; SD=1.634 mm) and the unburnt bones ($\bar{x}$=4.951 mm; SD=1.460 mm). On the other hand, at 800°C the mean kerf depth of the burnt bones was 3.280 mm (SD=0.545 mm), which is significantly less (p=0.050) than the unburnt bones with mean of 3.590 mm (SD=0.332 mm) (Figure 12 and Table 8).

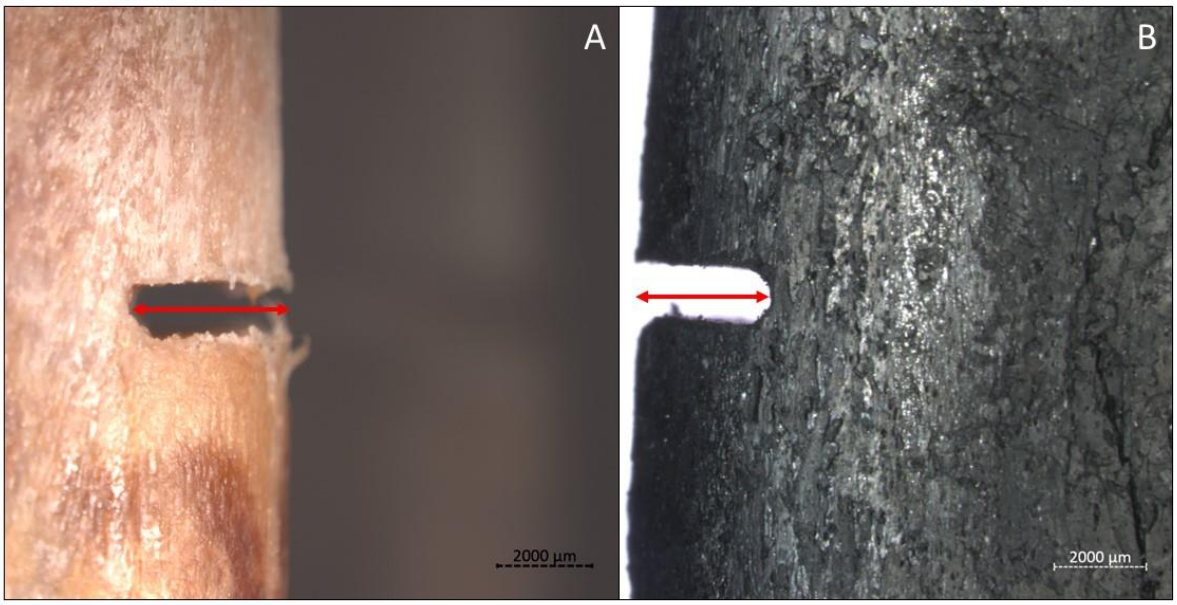

Figure 11: The kerf depth of incomplete lesions in A) unburnt and B) burnt bone.

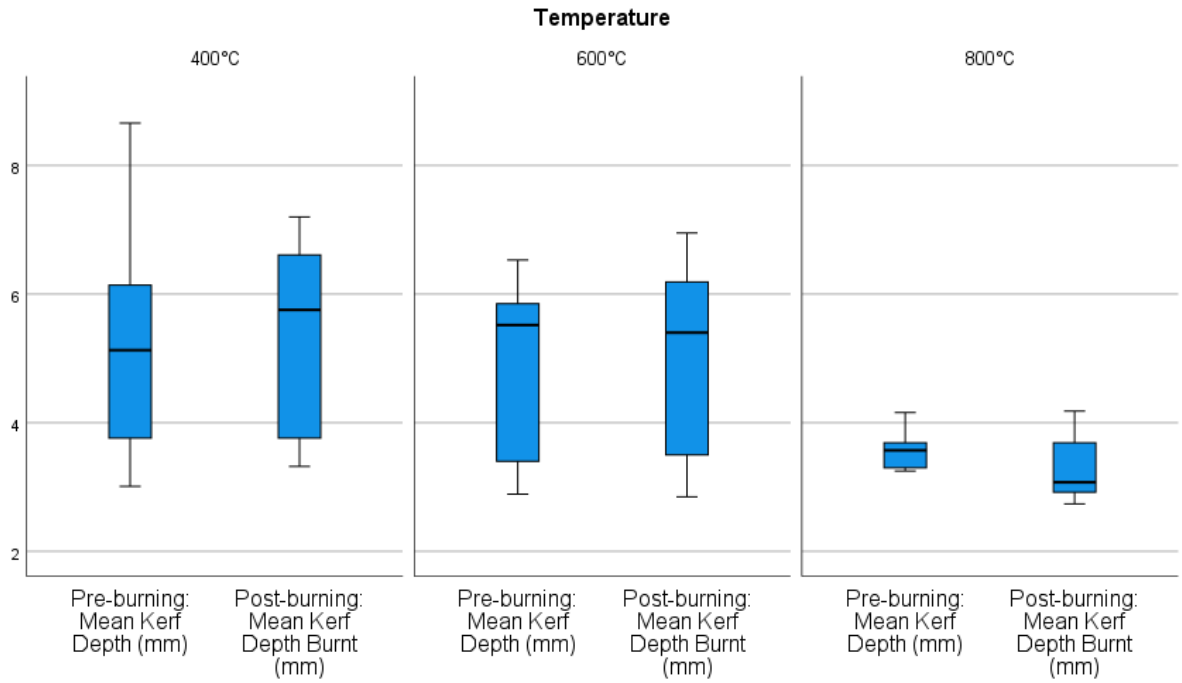

Figure 12: Box plots of incomplete cut kerf depths (millimetres) before and after burning in each burn temperatures groups.

3.4.2 Exit chipping, harmonics & bone islands

Overall, 1/18 (5.6 %) of the unburnt bones presented chipping, while only 2/18 (11.1 %) of the bones presented chipping after burning had taken place. Exit chipping was absent on the bone specimens before burning, and after burning at 400°C and 600°C, chipping was identified one out of six in each temperature group. Prior to burning at 800°C, one out of six bones showed exit chipping; however, after burning exit chipping was absent (Table 8).

Only one out of 18 bone specimens exhibited harmonics pre-burning; however, after burning the bone at 600°C, harmonics were absent. In the other temperature groups (400°C and 800°C), no harmonics were present pre- and post-burning.

No bone islands were present pre-burning and or post-burning across all temperature groups.

3.4.3 Profile shapes

Overall, 18/18 (100%) of the unburnt bones were round shaped whilst the burnt bones presented 16/18 (88.9%) round shapes and 2/18 (11.1%) were square with rounded corners.

All six round shaped profiles were identified in unburnt bones, and after burning at 400°C, five out of six were remain round shaped, while one was square with round corner shaped (Table 8). In the 600°C burn group, six unburnt bones exhibited round shapes, and after burning similar to the 400°C burn group, five out of six were identified to be round shaped while one showed the shape of a square with rounded corners. At the 800°C burn group, all of the six bones were round shaped pre-burning, and remained the same after burning.

Table 8: Mean measurement and presence of saw characteristics of incomplete cuts.

Characteristic	400°C		600°C		800°C		Total cuts analysed
N=18	**Pre-burning**	**Post-burning**	**Pre-burning**	**Post-burning**	**Pre-burning**	**Post-burning**	**Per Temperature group**
Mean Kerf width (mm)	1.150 mm	1.194 mm	1.148 mm	1.150 mm	1.182 mm	1.353[a] mm	6
Kerf depth (mm)	5.306 mm	5.400 mm	4.950 mm	5.048 mm	3.590 mm	3.280[a] mm	6
Exit chipping	0	1	0	1	1	0	6
Harmonics	0	0	1	0	0	0	6
Bone island	0	0	0	0	0	0	6
Profile shape	6 Round-shapes	5 Round-shapes 1 Square with round corners	6 Round-shapes	5 Round-shapes 1 Square with round corners	6 Round-shapes	6 Round-shapes	6

[a]shows statistical significance ($p < 0.05$) between pre-burning and post-burning in kerf width and kerf depth.

3.5 Complete transections

3.5.1 Breakaway spurs

Breakaway spurs were present in all the unburnt bones, and survived post-burning (Figure 13).

The mean thickness of breakaway spur for the unburnt bones was 1.635 mm (SD=0.608) and after burning at 400°C was 1.336 mm (SD=0.59505). This showed a statistically significant difference between unburnt and burnt bones (p=0.013). For the 600°C, there was no significant difference (p=0.424) between the unburnt ($\bar{x}$=1.60 mm; SD=0.317 mm) and burnt ($\bar{x}$=1.542 mm; SD=0.394 mm) bones. At 800°C, the mean thickness for the unburnt bones was 1.826 mm (SD=0.185 mm) which was significantly greater (p=0.001) than that of the burnt bones ($\bar{x}$=1.141 mm; SD=0.529 mm).

The mean length of breakaway spurs ($\bar{x}$=1.231 mm, SD=0.759 mm; $\bar{x}$=1.267 mm, SD=0.926 mm; $\bar{x}$=1.040 mm, SD =0.353 mm) in bones pre-burning showed no significant differences to

the mean length of bones post-burning at temperatures of 400°C ($\bar{x}$=1.254 mm; SD=0.729 mm p=0.823), 600°C ($\bar{x}$=1.229 mm; SD=0.554 mm; p=0.840) as well as 800°C ($\bar{x}$=1.058 mm; SD=1.0583 mm; p=0.903) (Table 9).

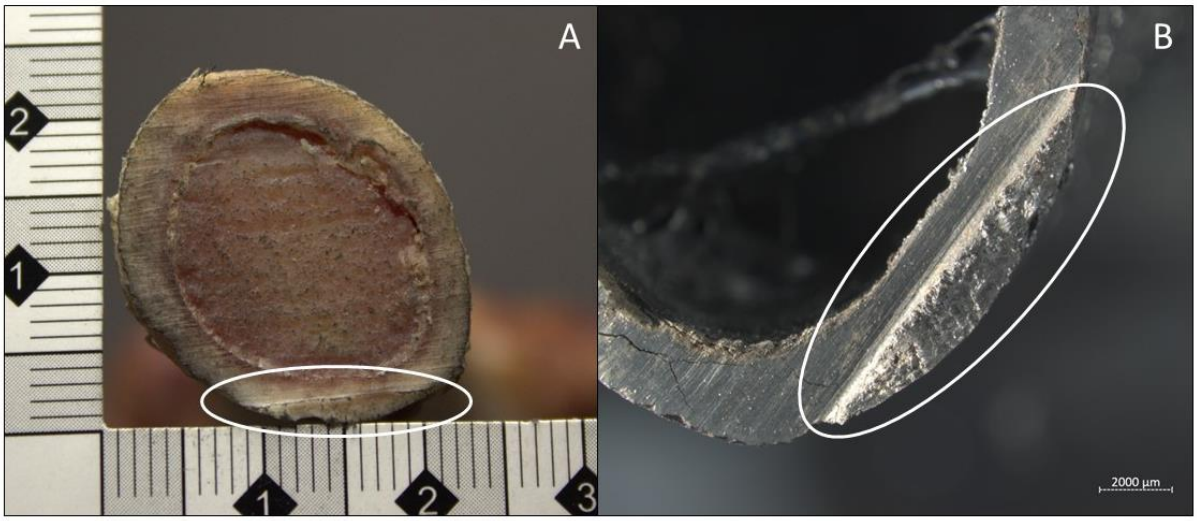

Figure 13: The breakaway spur of a complete cut on A) unburnt and B) burnt bone.

3.5.2 Pull-out striae

Pull-out striae were present in 5/36 (13.9%) bone specimens before burning and 6/36 (16.7%) present after burning (Table9).

Pull-out striae were visible in one cut surface prior to burning but following burning at 800°C, the pull-out striae were no longer visible. On the other hand, two cut surfaces was only revealed after burning at 400°C and 800°C (one per group). Altogether, there were 4/36 (11.1%) cut surfaces that remained before and after burning across all temperatures (Figure 14 & 15).

For the 400°C, no significant difference between the unburnt and burnt bones (p=0.249) were observed, although prior to burning there were 11 striae ($\bar{x}$= 0.403 mm) and following burning there were 13 striae ($\bar{x}$=0.643 mm). At 600°C, six striae were identified on the cut surfaces before burning with average distance of $\bar{x}$=0.7 mm. This shows no significant difference (p=0.339) to burnt bones with two striae observed on the cut surfaces, thus no measurement could be taken. Four pull-out striae (average distance of $\bar{x}$=0.235mm) were observed before burning the bones at 800°C. After burning, six striae were observed (average distance of $\bar{x}$=0.225mm) and no significant differences were found (p=0.936).

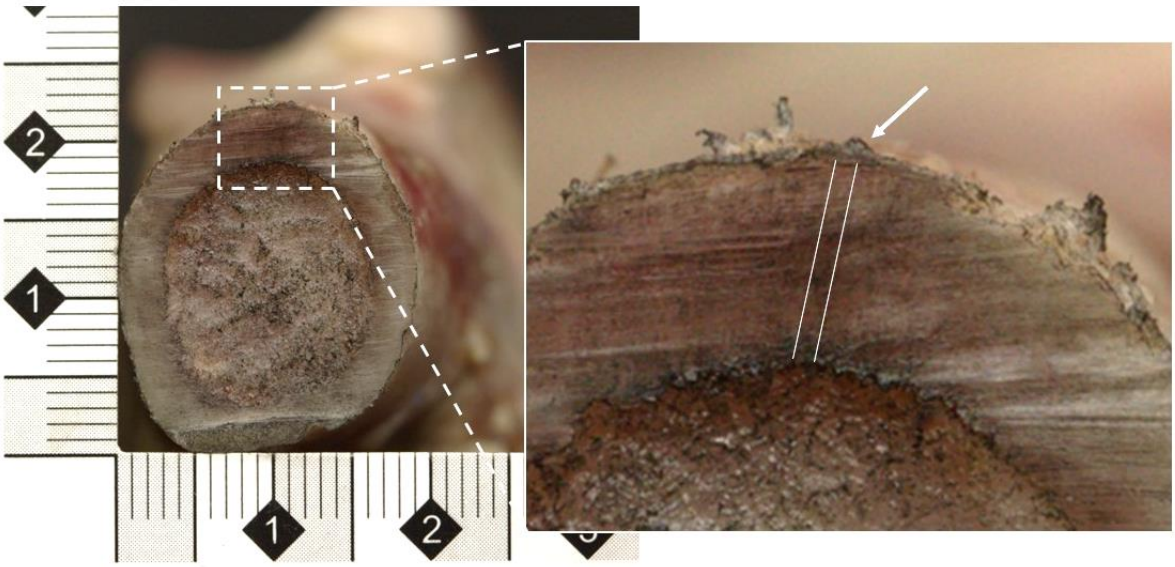

Figure 14: Pull-out striae before burning.

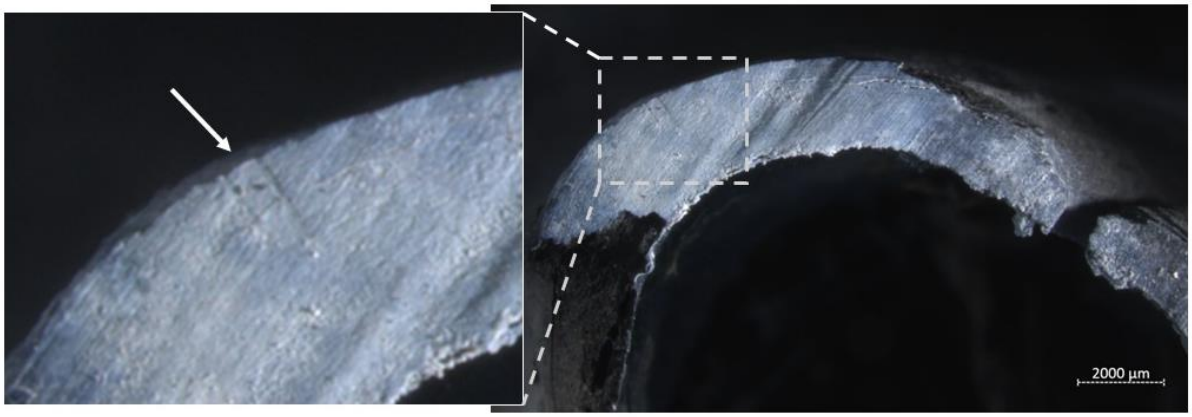

Figure 15: Pull-out striae after burning.

3.5.3 Striations regularity

In general, the 36 cut surfaces displayed the same non-uniform striations before and after burning across all temperatures (400°C, 600°C and 800°C).

The distance between striations were significantly different ($p<0.001$) when comparing the bone specimens pre-burning and post-burning at 400°C, 600°C and 800°C (Table 9). The average striation distances pre-burning was $\bar{x}$=0.090 mm (SD=0.018 mm), and decreased to $\bar{x}$=0.061mm (SD=0.148 mm) after burning at 400°C. For the 600°C, pre-burning measurement was $\bar{x}$=0.085 mm (SD=0.0129 mm) and after burning was $\bar{x}$=0.055mm (SD=0.015 mm). The

average distance for the 800°C group prior to burning was $\bar{x}$=0.086 mm (SD=0.017 mm), and after burning, decreased to $\bar{x}$=0.057 mm (SD=0.008 mm) (Table 9 and Figure 16).

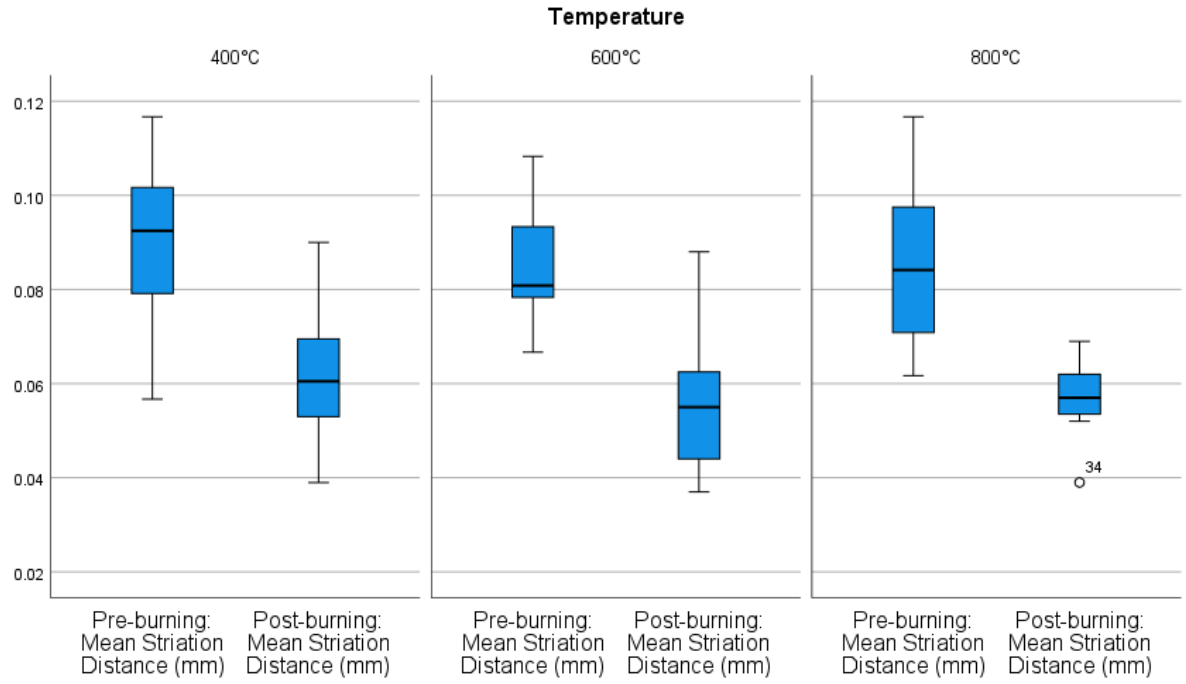

Figure 16: Box plots of mean striation distance (millimetres) of complete cuts before and after burning in each burn temperatures groups.

3.5.4 Exit chipping, harmonics and tooth hops

Exit chipping was found overall in 35/36 (97.2%) of the unburnt bone specimens and after burning at 400°C, 600°C and 800°C, decreased to 26/36 (72.2%) (Figure 17). The presence of this characteristic per temperature can be seen in Table 9. Nine out of 36 unburnt cut surfaces exhibited exit chipping and were not observed after burning across the burn temperature groups. As an exception, a single bone specimen did not show exit chipping, which was observed in the 800°C burn group.

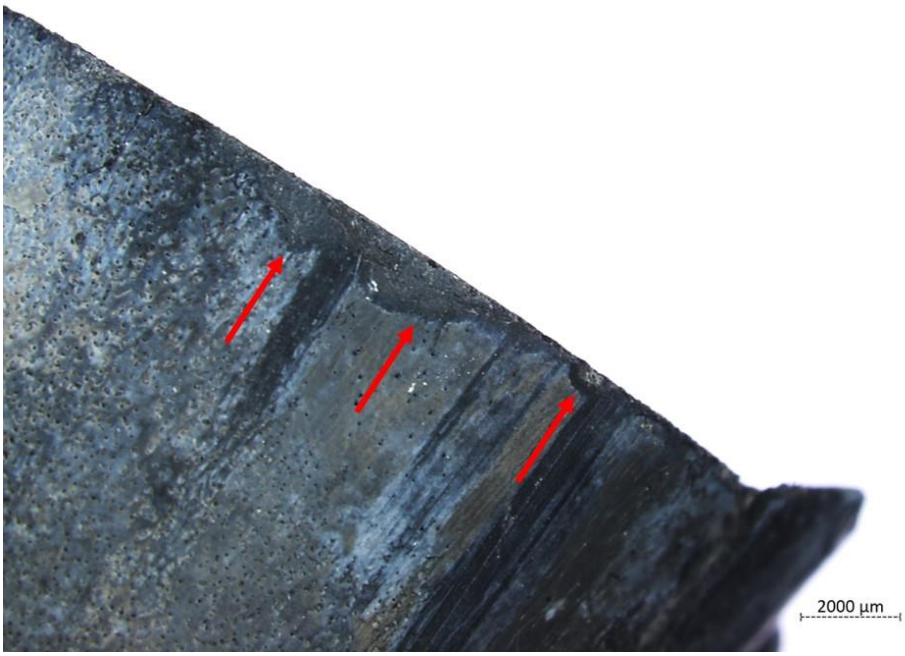

Figure 17: Exit chipping identified on a complete cut of a burnt bone.

Harmonics were present in 7/36 (19.4%) of the unburnt and burnt specimens. Harmonics were minimal, with four out of 36 present post-burning and found across all temperature groups, while it was not identified pre-burning. Four cut surfaces exhibited harmonics, but harmonics were absent after burning at 800°C. Three cut surfaces remained the same before and after burning at temperatures of 600°C and 800°C.

Tooth hop was present in 9/36 (25%) unburnt bone and decreased to 4/36 (11.1%) after burning. Tooth hop (6/36) was identified in the cut surfaces of the bone sample before burning but was dissipated after burning (in the 600°C and 800°C group) (Figure 18 and 19). One cut surface did not have tooth hop, however, after burning at 800°C this characteristic became visible. Three out of 36 cut surfaces presented as having tooth hop prior to burning and remained the same post-burning.

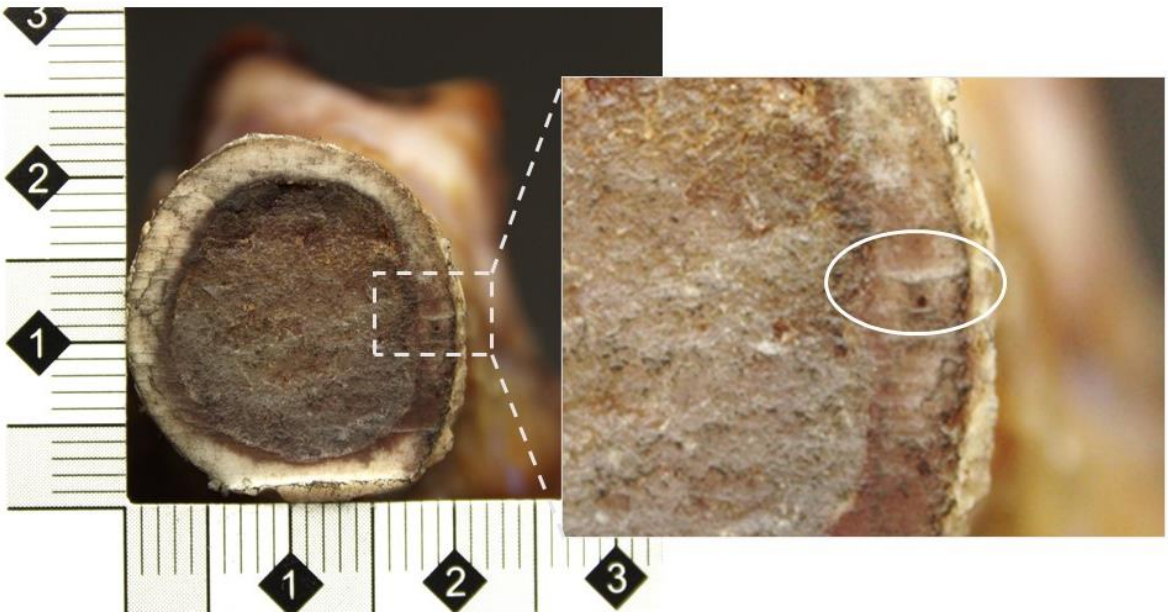

Figure 18: Tooth hop present on bone before burning.

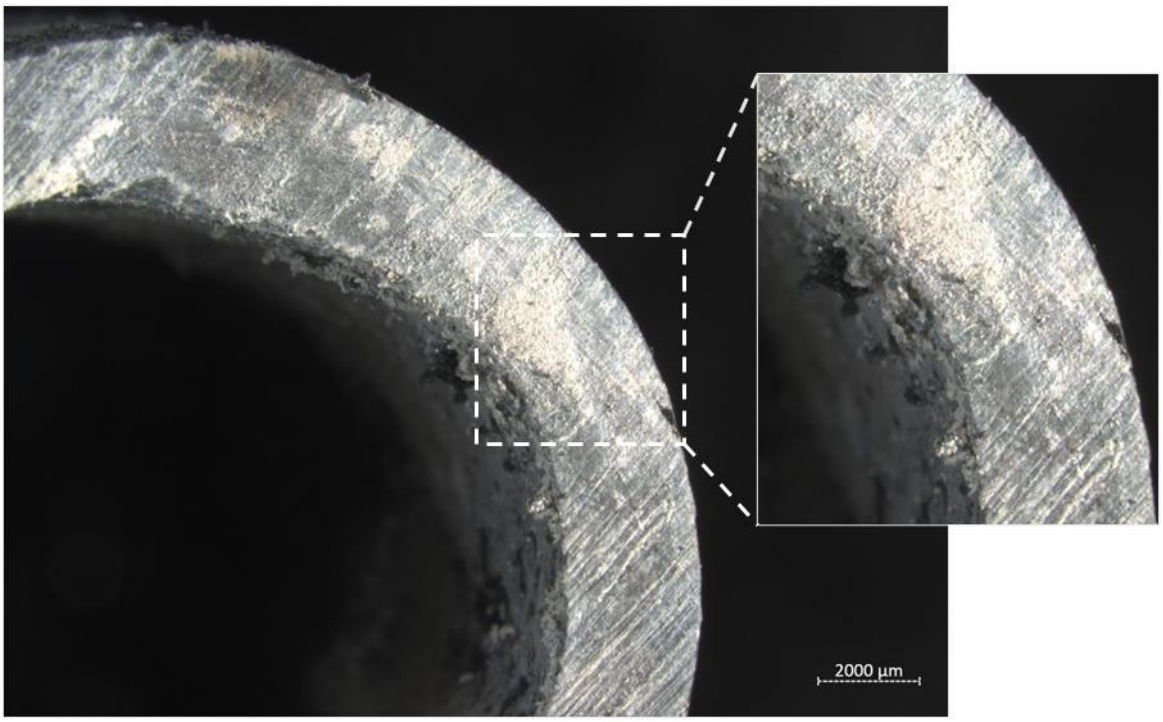

Figure 19: Tooth hop absent on bone after burning.

Table 9: Mean measurement and presence of saw characteristics of complete transections.

Characteristic	**400°C**		**600°C**		**800°C**		**Total cut surface analysed**
N=18	**Pre-burning**	**Post-burning**	**Pre-burning**	**Post-burning**	**Pre-burning**	**Post-burning**	**Per Temperature group**
Breakaway spur presence	12 (100%)	12 (100%)	12 (100%)	12 (100%)	12 (100%)	12 (100%)	12
Breakaway spur thickness (mm)	1.635 mm	1.336[a] mm	1.60 mm	1.54 mm	1.826 mm	1.141[a] mm	12
Breakaway spur length (mm)	1.231 mm	1.254 mm	1.267 mm	1.229 mm	1.040mm	1.058 mm	12
Number of Pull-out striae present	11	13	6	2	4	6	12
Pull-out striae Mean distance	0.403 mm	0.643 mm	0.7 mm	0 mm	0.235 mm	0.225 mm	12
Striation regularity	Non-Uniform	Non-Uniform	Non-Uniform	Non-Uniform	Non-Uniform	Non-Uniform	12
Striation mean distance	0.090 mm	0.061[a] mm	0.085 mm	0.055[a] mm	0.086 mm	0.057[a] mm	12
Exit chipping	12 (100%)	11 (91.7%)	12 (100%)	10 (83.3%)	11 (91.7%)	5 (41.7%)	12
Harmonics	0 (0%)	2 (16.7%)	2 (16.7%)	2 (16.7%)	5 (41.7%)	3 (25%)	12
Tooth hop	3 (25%)	3 (25%)	2 (16.7%)	0 (0%)	4 (33.3%)	1 (8.3%)	12

[a]$p < 0.05$ shows significance between pre-burning and post-burning of the thickness and length of breakaway spurs, distance of pull-out striae and the distance between the striation patterns.

CHAPTER 4: Discussion

The primary aim of this study was to analyse and compare morphometric and morphologic differences in saw mark trauma before and after burning at various controlled temperatures. This study analysed 54 saw marks on 18 de-fleshed lamb femur bones that were created using a back/tenon saw through manual infliction by one individual. Interpretations of these results, further research improving the experimental design, limitations and future improvements are discussed below.

In a forensic case involving criminal dismemberment, it is often most challenging to distinguish sharp force trauma from heat-induced fractures (Herrmann & Bennett, 1999; Vachirawongsakorn, Painter & Márquez-Grant, 2022; Vegh & Rando, 2019). Heat-induced alteration on bones eventually affects the analysis of sex, age, stature, ancestry as well as the trauma inflicted before and after burning (Ellingham et al., 2015; Marciniak, 2009; Pope & Smith, 2004; Thompson, 2005). In cases where a body is subsequently burned there could be alteration to the trauma leading to the concealment of trauma.

As mentioned previously saws can create marks in many ways on the bone, which is dependent on multiple factors. However, it has been established that saw mark characteristics found on bones can act as useful markers for the identification of the class of saw used (Berger et al., 2018; Nogueira et al., 2016; Symes et al., 1992, 2010). It becomes challenging to analyse burnt bones, but in spite of this, microscopic assessment of the morphology, colour assessment and examination of the crystallin structure may shed light on the maximum temperature reached in the process of burning the bones.

Thus, further research is needed to discover the effects of burning on saw class characteristics, considering the planning and execution of such an experiment as well. It is essential to detect the visibility of toolmarks that may have survived on bones that have been exposed to heat for forensic purposes. In general, previous research by Symes et al. (1992, 2010) has found that bone cuts exhibit features of the type of tool used to create the lesions; the effects of heat on these features, as examined by various authors, were compared to the present study. In this study, analysis of the bones and how thermal changes took place as well as saw mark characteristics will be highlighted.

4.1 Experimental design and conditions

Previous literature on trauma morphology have utilised a variety of animal models. Typically, research had been conducted on porcine bones, however, Nogueira et al. (2018) caution the use of only pig bones as the authors found significant differences to human bones when comparing trauma morphology specifically in false start lesions. An alternative could be lamb (*Ovis aries*) femur bones (Dittmar, Errickson & Caffell, 2015; Macoveciuc et al., 2017; Reber & Simmons, 2015; Saville, Hainsworth & Rutty, 2007; Shipman, Foster & Schoeninger, 1984; Thompson, 2005).

Lamb femur bones were chosen as a model in this study due to the similarity of shape and bone structure when compared to human femur bones. Additionally, studies on the fracture mechanics between human and lamb femur bones have promoted the use of lamb bones as analogues for human bones (Dempsey et al., 2019; Reber & Simmons, 2015). The femur bone is a common area at which dismemberment of a limb occurs (Reichs, 1998), yet another reason for the use of femur bones in this research. Macoveciuc and colleagues (2017) also looked at thermal alteration on burnt sheep bones; therefore, results from their research can be compared to the current study.

The ease of availability of lamb bones and structural similarity to humans make it a good model, however age of the bone should be taken into account when analysing results. Bone composition varies with age, making it a possible limitation as it can affect the different saw marks and fragmentations. Thus, it is essential to compare different age groups in order to obtain more accurate findings.

Waterhouse (2013) stated that younger bones are more flexible when compared to older bones, which leads to less fragmentation. Juvenile bones differ greatly from adolescent bones with regards to elasticity which affects the mechanical weight and stress before a defect is created. The elasticity in adult bones is more mineralised and would mean that most organic compounds are lost during the process of burning. As such, these bones undergo less shrinkage and consequently less heat-induced fractures occur (Robbins, Fairgrieve & Oost, 2014). Therefore, the ability of the bone to withstand force by sharp force trauma is not the only factor to consider, but also the age of the bone. Both these factors influence the degree to which bone can resist alteration or damage by heat (Marciniak, 2008).

A further consideration in trauma and/ or burn studies is the choice of using fleshed or de-fleshed bone samples. De-fleshed bones were chosen because it was easier for visual assessment and the burning process. The skin, muscles and fat acts as fuel and can affect the

selected temperature at which the bones are burnt. Even though it does not mimic the reality forensic burn scenarios, the soft tissue removed from the bones ensures that the temperature is spread across the specimens evenly and also allows assessment of trauma before burning (Macoveciuc et al., 2017) and may provide standardised results for future research.

Only a few studies have been conducted in which temperature is a controlled variable used to determine the exact changes in physical alterations and morphological changes on the bones. While outdoor fires replicate a real-life scenario, interpretation of the effects of specific temperature and burning duration of bones, cannot be adequately inferred. Thus, in order to gain a clearer understanding of the effects of fire on sharp force trauma in bones, it is necessary to use a controlled setting.

Controlled temperatures would allow for consistent and repeatable experimental conditions and the results thereof could be compared to outdoor fire results. It would be easier to examine the outcomes of bones burnt in with controlled temperature and to identify which effects or factors have influenced the bone evidence observed; a controlled setting would also possibly enable the deduction of the maximum temperature of a fire-related scenario. In this way, studying bone evidence samples across varied controlled temperatures settings would contribute to existing literature.

In this study, when bones were exposed to controlled and evenly distributed temperatures using an electric furnace, as expected, the colour of the bones appeared uniform and no differential burning was observed. In contrast, an open fire setting would have irregular burning patterns or burn line fractures. This shows partial exposure of the bone to the fire with a line separating unburnt from burnt surfaces (Symes et al., 2008).

4.2 Casts

In forensic literature, casts are useful for analysis and characterisation of bone trauma (Bernandi et al., 2019; Collord-Stalder, 2020; Nogueira et al., 2016). The profile shapes of the false start lesions were obtained from casts, in this current study. This method was preferred as the false start lesions on the bones were too small to assess. For this reason, the shape was derived from ‘negative’ or ‘reverse’ casts similar to previous studies by Dittmar, Errickson & Caffell (2015) and Nogueira et al. (2018). Similar to Bernandi et al. (2019), this study also analysed kerf depths of false starts and incomplete cuts from casts. Also, the use of a stereomicroscope allowed for better visualisation and classification of the casts to analyse the characteristics.

A consideration should be taken when analysing profile shapes from casts. When the casting material is applied onto the false starts, the mold takes the shape of what the lesions are, including if there are cracks or bone debris from sawing and/ or burning. This can possibly alter the profile shape when casts are peeled from the bone and analysed, which could infer inaccurate information to match to the tool used to create the lesions. Therefore, it is recommended to compare casts and the physical bone lesions.

In general, the application of casts on the bones, whether fresh or unburnt, was relatively easy. Peeling casts from burnt bones was particularly challenging, as some of the superficial bone layer stuck to the casts and could potentially ruin or destroy the identifying features of a saw mark. When applying casts, it is essential to handle bones burnt at 800°C with care, as they are particularly fragile. Therefore, this cast application should be done as the last step in case of accidental fragmentation in burnt bones.

Overall, casts helped support the collection of data especially in false starts and incomplete cuts. In agreement with the study by Nogueira et al. (2016), using casts was easier, and could potentially be the best way to analyse these types of saw marks, as it might be impossible to use measuring tools directly onto the bones (fresh or burnt).

4.3 Thermal alteration: colouration and fractures

In a forensic case context, it is more likely that a dismembered body would initially still have soft tissue when exposed to fire; this tissue would then act as a protective layer against heat. Also, when injuries caused by sharp force trauma occur, these would lead to open wounds which expose the inner layers of the bones and can affect the colour change (Pope & Smith, 2004). In agreement with authors Pope & Smith (2004) and Thompson (2005), it would be better to state that temperature is not an indication of how the colour appears, but rather that decomposition of the organic compartments of the bone indicated how colours will appear.

As described in the introduction, a gradual change in colour of bone is observed as temperature of burning increases. Colour changes in bone observed in this study did not deviate from previous research (Alunni et al., 2017; Ellingham et al., 2015). The bones in this study underwent carbonisation which produced a black colour in bones at 400°C and 600°C burn temperatures. In the 800°C group thermal decomposition reached the early stages of calcination, but bones were still carbonised. In contrast to Symes et al. (2012) study, the authors found that bones reached the calcined stage at 500°C, except that the burn duration was longer (90 minutes).

When comparing the unburnt bones, the different cut types can easily be identified with no fragments or cracks present, even after burning. Burning creates distortion and warping, thus able to induce bone fractures. Heat-induced fractures were evident on all of the samples, in the present study. From previous literature, bone fractures may radiate further along the bone shaft or even increase in depth from pre-existing fractures when exposed to heat (Macoveciuc et al., 2017). Fractures appeared to originate from the base of the saw mark or longitudinally split across the saw mark. Fractures formed from pre-existing saw marks were notably different from heat-induced fractures. Therefore, saw marks remained visible across the different controlled temperatures, except for one bone specimen that did not display a false start lesion after burning in at 800°C. The absence of this cut could be attributed to the process of delamination.

Delamination is defined as the process by which the cortical layers of the cancellous bones are fractured and split away – the cancellous bone on the epiphyses is exposed (Symes et al., 2008). Relating to a forensic scenario, false start lesions could be lost in evidence recovery as the bones are brittle and fragile, especially when exposed to very high temperatures (800°C) as seen in the current study. Heat alteration of bones can occur at any stage of the burning process; however, it is primarily determined by the duration of burning and temperature intensity (Symes et al., 2008). Also, during collection, transport and analysis, the bones fragment easily which could destroy evidence of bone trauma compromising the value of burnt bones as evidence (Mata-Tutor et al., 2021a).

Signs of heat alteration in saw marks were also seen at the kerf floor which was split or cracked further apart and warped. When comparing the 400°C, 600°C and 800°C burn temperature groups, it was observed that most fractures occurred in the 800°C burn group Specifically, longitudinal fractures were most common followed by the other fracture types including curved transverse, transverse, step, patina, delamination and splinter fractures. The different types of fracture patterns were harder to differentiate, as temperature increased.

Across all temperatures, the longitudinal fractures, displayed some cracking perpendicularly across false starts and incomplete cuts. In contrast to the current study, Marciniak (2008) found that false starts did not manifest any heat-induced fragmentations or fractures. A possible reason for this could be the presence and protective nature of soft tissue on the bones. Therefore, clear understanding of interpretation of bone fracture patterns is essential in the forensic crime scene.

4.4 Thermal alteration: saw mark characteristics

In this study, most characteristics on burnt and unburnt bone were macroscopically observable; however, the addition of oblique lighting and contrast in the form of black fingerprint powder aided visualisation in unburnt bones (Isa et al., 2021). Fingerprint powder was not necessary in burnt bones; the oblique lighting enhancement technique (Isa et al., 2021) was used on the surface area of bones having a dark blackened colour which aided in the visualisation of characteristics. The stereomicroscope enhanced visual characteristics and provided additional information on various other characteristics found.

The saw mark characteristics such as pull-out striae, striation regularity and specifically exit chipping were visibly enhanced post-burning in this study; similar to previous literature (Macoveciuc et al., 2017; Robbins, Fairgrieve & Oost, 2014; Symes et al., 2010). Contrary to these findings, Kooi & Fairgrieve (2013) stated that cut mark characteristics were more visible on fresh bones. The authors mentioned that characteristics are often destroyed by burning, for example, the occurrence of fragmentation or removal of soft tissue during the burning process.

Post-burning observation performed on the saw marks which were present before burning, suggest that these marks were lost during the burning process namely: exit chippings and harmonics, which were present on the incomplete and complete transections but were absent after burning at 600°C and 800°C. Pull-out striation in the complete transections was absent after burning at 600°C. Additionally, tooth hops disappeared at 600°C and 800°C burn temperatures. The loss of characteristics post-burning, occurred most frequently at the highest temperature, suggesting that thermal damage increases as temperature rises.

Interestingly, several characteristics which were absent pre-burning, were revealed post-burning. Exit chipping was absent on incomplete cuts; however, these appeared after burning at of 400°C and 600°C. Harmonics appeared after burning at 400°C and 800°C, while pull-out striae and tooth hop only at 800°C. The reason for these occurrences could be due to the bone marrow present as a layer obscuring the cut surface of unburnt bone. The layer of bone marrow could have been created by blade interaction with the bone - the ‘lifting’ and ‘insertion’ or the ‘forwards’ and ‘backwards’ motion of the saw, picks up the marrow and created an extra layer on the bone surface. In addition, the colour of the bones before and after burning were contrasting, which could have influenced the visibility of the bone characteristics. Also, the gradual dehydration of the bone during burning can also impact the saw mark characteristics - as the bone loses moisture, the characteristic becomes pronounced leading to enhanced visibility.

Striations are common saw mark characteristics found along the kerf wall which are created by the sawing action onto bones. Symes and colleagues (2010) noted that hand powered saws tend to have different striae regularity compared to mechanically powered saws which reproduce more consistent or uniform striae. In this study, the non-uniform striae on all the bones were retained, and clearer after burning across all temperatures. Marciniak (2008) also found that saw mark striae were more noticeable after samples were burnt, however, the temperature did not exceed 400°C in an outdoor fire. According to Marciniak (2008), the minimal post-burning damage on striae is possibly due to minimal change in the macroscopic structure of bone when bones are at the stage of carbonisation and pyrolysis.

The average distance between each pull-out striae observed in this study was not a true representation of the distance of pull-out striae. This is on account that the number of pull-out striae identified are not always found next to one other on the cut surface, which could lead to a measurement error. In agreement with Martlin & Rando (2020), error when measuring pull-out striae will be greater if the tooth set is unknown.

Although the effort to maintain the same consistent force and angle were applied onto the back/tenon saw, to create the saw marks, each mark observed was slightly different in width size and occasionally in shape. Even so, the findings of the saw mark dimensions exposed to heat are consistent with previous studies (Herrman & Bennet, 1999; Robbins, Fairgrieve & Oost, 2014; Symes et al., 2012). The saw mark size was mostly preserved after burning and differed minimally with an increase average of 0.061 mm in false start lesions and 0.075 mm for incomplete cuts, across all temperatures.

The kerf widths were found to expand following burning - this can be explained by the expansion of the bone due to heat, which was significant at 800°C. As the temperature increased, the bones started to warp and deform. At 800°C, one false start lesion measurement could not be collected as the bone broke at the lesion, thus preventing an accurate measurement. This information is comparable to the selected temperature of this study and supported by the results found by Vegh and Rando (2019) in which kerf width also expanded post-burning at 300°C, 600°C and 1000°C, but metrically (0.15 mm) differs slightly.

In relation to profile shapes, as expected, 97.2% round shaped kerf floors were identified in unburnt false start and incomplete lesions, and after burning, decreased to 75%. In the 400°C and 600°C, the number of shapes that changed from round shapes to square with rounded corners, were consistent. Most changes occurred in the 800°C group, suggesting that from this degree and higher it is more challenging to analyse profile shapes, especially the false start

lesions. As mentioned, a possible reason could be due to the casting process, where the casts can take the shape of the debris found in the lesions and when analysing the cast, another shape could be identified.

The shape of the kerf walls was evaluated for the type of teeth set used to create the lesions. The saw utilised in the current study has a TPI of 13 and alternating tooth set. In all false start lesions, the shapes were all found to be straight. Despite this, Symes et al. (1992) stated that alternating teeth sets would create narrow to wide patterns. Bernardi et al., (2020) confirmed this and showed that alternating saws created narrow and wide parts in false start lesions on pig and human bone samples. However, the authors also found that it was possible to have straight walls; this would happen when the blade had not penetrated deep enough into the bone.

In contrast to Bernandi et al. (2020), Nogueira and colleagues (2016) found that human bones often presented straighter walls than pig bones. Nevertheless, these studies showed that alternating saws can create straight walls. The degree of alteration and size of the teeth was relatively small on the backsaw used for the current study, which may have contributed to creating straight walls. This could mean that a more comprehensive analysis of the shape of the walls of false starts on sheep bones to human bones is necessary.

Investigating the presence or absence of saw mark characteristics contributes to saw mark analysis overall. The type of blade may give all or some characteristics; thus, it is important to note any significant findings. Bone islands were absent in all bone specimens, which attributes to the straight cuts found in all kerf floors of the false start lesions. In line with Nogueira et al. (2018), no bone islands were produced from alternating saws. The false start lesions were possibly too shallow as the teeth may have not penetrated the bone at a depth conducive to the creation of bone islands. Furthermore, a larger teeth set is more likely to create bone islands (Nogueira et al., 2018). On the contrary, Symes et al. (2010), stated that alternating teeth sets have been found to create bone islands.

Symes et al. (2012) found exit chipping had decreased post-burning at 500°C and similar to this study, exit chipping decreased more as the burn temperature increased. Exit chipping can help determine directionality of a saw used in dismemberment cases, but apart from this, it is important to know the fundamentals of saw mark characteristics and how bone undergoes heat alterations in order to differentiate characteristic similarities. For example, it was found that exit chipping in this study, resembled bone delamination in the higher burn temperatures. In the 800°C temperature group, absence of exit chipping was mostly due to the difficult process of identification as most were burnt off; also, most fractures occurred in this group. For the

complete transections, fractures caused many small broken pieces, which made it harder to identify this characteristic.

Harmonics, which can be used to identify TPI (Symes et al., 2010), were present in the complete transections only. This suggests that the more the saw interacts with the bone the more chances there are to divert from angle and force consistency. Hence, the incomplete lesions were absent of harmonics, due to less contact of the saw interacting with the bone. Furthermore, previous researchers (Berger et al., 2018; Symes et al., 2010) denoted that alternating blades most often create harmonics and is created directly from a normal cutting action; however, this characteristic was minimal across all temperature groups.

In all temperature groups, the breakaway spur length did not change drastically, indicating that this characteristic can still be obtained after high heat exposure. The size of the breakaway projection is dependent on the energy expended onto the bone during cutting (Berger et al., 2018). The breakaway spur may also assist in identifying the directionality of the saw blade used and how the perpetrator might have placed the body during dismemberment (Hackman & Black, 2017; Symes et al., 1992).

The breakaway spur thickness in the 600°C burn group did not differ significantly from that observed in the 400°C and 800°C burn group. Bones burnt in the 600°C group could have been unaffected by the handling or placement of bones during the burning and assessment procedures.

Tooth hop was less prevalent in burnt bones than in fresh bones, in this study, which is contrary to the results found by Robbins, Fairgrieve & Oost (2014). However, Berger et al. (2018) mentioned that tooth hops were too few for an accurate statistical analysis to be performed, which is in agreement with the current study, but contrary to the findings of Love et al. (2014). Similarly to pull-out striae, tooth hops were also observed under oblique lighting. It is evident that heat exposure altered or obliterated certain characteristics. Therefore, as hypothesized, increased temperatures are proportionate to thermal damage on bones.

4.5 Limitations, improvements and future research

This study has provided preliminary data on the effect of heat exposure to pre-existing saw mark trauma on bone. This study is part of a larger ongoing research project. As such only one duration of burning (20 minutes) was investigated. Beyond the immediate study there is also scope for future research investigating further burn durations at the same temperatures, different type of saws potentially used to inflict bone trauma and bone types. Additionally, the

use of SEM in previous literature has been shown to provide enhanced imaging capabilities on minute characteristics on unburnt or burnt bones, characteristics which may not be visible to the naked eye or with the use of stereomicroscope (Alunni et al., 2018; Dittmar, 2017; Kooi & Fairgrieve, 2013). This method was unfortunately beyond the scope of the current study and will also be included in future research.

Further effort also needed improve the validity of collecting metrics on saw marks. Stereomicroscopy was sufficient to analyse saw marks and relatively cheaper than other advanced microscopic analysis. However, characteristics not clearly observed using the stereomicroscope in this study, can undergo the same assessments using SEM. Thereafter, the future results obtained from SEM examination could be analysed and compared to the results of this study. Furthermore, SEM can be minimally invasive and function as a useful tool to confirm the presence of a characteristic (Kooi & Fairgrieve, 2013; Ubelaker & Wu, 2020).

It should be noted that the results obtained in this research was only tested for one particular saw (back/tenon saw). Hence, a possible limitation to interpreting the results may differ to used saws. Typically, when sharp force trauma studies are carried out, newly purchased tools are used with less defects rather than used tools (Norman et al., 2018a). For this reason, further research is necessary to determine the effect of tooth wear on saw mark characteristics.

Lastly, femur bones were the only type of bones used in this study; although the majority of dismemberment takes place on this type of bone (Marciniak, 2008), there are other bones to take into consideration as well. The femur bone is capable of resisting more force and possess the ability to retain saw mark characteristics more effectively, even when exposed to heat. The femur shaft can also be compared to the epiphyses of the bone as the heat may impact the bone structure differently. Furthermore, the bone density of femur bones may differ from other bones (Marciniak, 2008), thus making the comparison to different bone types and the impact of saw mark trauma on these bones worthy for future research.

Conclusion

The present study investigated saw mark morphology on sheep bones and was carried out in a controlled laboratory environment. The characteristics burnt in each temperature group were slightly different, but the pattern is apparent that the bone specimens experienced a greater degree of alteration as the temperature increased. For example, bone weight, kerf depth, exit chipping and tooth hop were either altered or obliterated most frequently at the highest temperature.

Heat-induced trauma could be macroscopically differentiated from the saw marks (false starts, incomplete cuts and complete cuts). Fracturing, discoloration, shrinkage and warping occurred most frequently in the 800°C temperature and made it complicated to measure and collect information.

From previous literature, saw mark characteristics are more often used to identify the type of saw used and less on matching to the tool after burning has occurred Overall, this study showed that the controlled temperatures of 400°C, 600°C and 800°C had an impact on the saw mark characteristics. This provides the building blocks for future research into on saw mark analysis and the effects of controlled heat exposure.

References

Alsop, K., Baier, W., Norman, D., Burnett, B. & Williams, M.A. 2020. Accurate prediction of saw blade thickness from false start measurements. *Forensic Science International*. 318:1-8.

Alunni, V., Nogueira, L., & Quatrehomme, G. 2018. Macroscopic and stereomicroscopic comparison of hacking trauma of bones before and after carbonization. *International Journal of Legal Medicine*. 132(2):643-648.

Baby, R.S. 1954. *Hopewell cremation practices*. Columbus, Ohio: Ohio Historical Society.

Berger, J.M., Pokines, J.T. & Moore, T.L. 2018. Analysis of class characteristics of reciprocating saws. *Journal of Forensic Sciences*. 63(6):1661-1672.

Bernardi, C., Nogueira, L., Cabusat-Mailliet, C., Carle, G., Alunni, V. & Quatrehomme, G. 2020. Analysis of false starts lesions on human bones produced by two hand saws with high TPI. *International Journal of Forensics*. 134:613-618.

Binford, L.R. 1963. An analysis of cremations from three Michigan sites. *Wisconsin Archaeologist*. 44: 98-110.

Blom, L., Van Niekerk, A. & Laflamme, L. Epidemiology of fatal burns in rural South Africa: A mortuary register-based study from Mpumalanga Province. *Journal of the International Society for Burn Injuries.* 37(8)1394-402.

Carroll, E.L. & Smith, M. 2018. Burning questions: Investigations using field experimentation of different patterns of change to bone in accidental vs deliberate burning scenarios. *Journal of Archaeological Science*. 20:952-963.

Castillo, R.F., Ubelaker, D.H., Acosta, J.A.L. & Cañades de la Fuente, G.A. 2013. Effects of temperature on bone tissue. Histological study of the changes in the bone matrix. *Forensic Science International*. 226:33-37.

Collini, F., Amadasi, A., Mazzucchi, A., Porta, D., Regazzola, V.L., Garofalo, P., Di Blasio, A. & Cattaneo, C. 2015. The erratic behavior of lesions in burnt bone. *Journal of Forensic Science*. 60(5):1290-1294.

Collord-Stalder, H.G. 2020. Digital microscopic methods for sharp force trauma in burned human and nonhuman remains. M.A. Dissertation. Texas State University.

De Gruchy, S. & Rogers, T.L. 2002. Identifying chop marks on cremated bone: a preliminary study. *Journal of Forensic Sciences*. 47:933–936.

Dittmar, J.M. 2017. Cut to the bone. In *Human Remains: Another Dimension*. D. Errickson & T. Thompson. Eds. London: Academic Press. 45-46.

Dittmar, J.M., Errickson, D. & Caffell, A. 2015. The comparison and application of silicone casting material for trauma analysis on well preserved archeoloigcal skeletal remains. *Journal of Archeological Science: Reports.* 4:559-564.

Ellingham, S.T.D., Thompson, T.J.U. & Islam, M. 2015. Thermogravimetric analysis of property changes and weight loss in incinerated bone. Palaeogeography, Palaeoclimatology, Palaeoecology. 438:239-244.

Ellingham, S.T.D., Thompson, T.J.U., Islam, M. & Taylor, G. 2015. Estimating temperature exposure of burnt bone – A methodological review. *Science and Justice*. 55:181-188.

Fanton, L., Jdeed, K., Tilhet-Coartet, S. & Malicier, D. 2006. Criminal burning. *Forensic Science International*. 158:87-93.

Feldman, A.D. 2015. From trauma to trial: proposing new methods for examining the variability of sharp force trauma on bone. M.A. thesis. San José State University.

Freas, L.E. 2010. Assessment of wear-related features of the kerf wall from saw marks in bone. *Journal of Forensic Sciences*. 55(6):1561-1569.

Grosso, A.R. 2022. Tooth hop variability in human and nonhuman bone: effect on the estimation of saw blade TPI. *Journal of Forensic Sciences*. 67(1):102-111.

Guilbeau, M.G. 1989. The analysis of saw marks in bone. M.A. thesis. The University of Tennessee, Knoxville.

Hackman, L. & Black, S. 2017. The role of forensic anthropology in cases of dismemberment. In *Criminal dismemberment: Forensic and investigative Analysis*. S. Black, G. Rutty, S.V. Hainsworth & G. Thomson, Eds. Dundee: CRC Press. 113-134.

Herrman, N.P. & Bennett, J.L. 1999. The differentiation of traumatic and heat-related fractures in burned bone. *Journal of Forensic Sciences*. 44(3):461-469.

Hughes, E. 2018. Variation of tool mark characteristics in frozen bone as it relates to dismemberment. Graduate Student Thesis. Dissertation. University of Montana.

Imaizumi, K. 2015. Forensic investigation of burnt human remains. *Research and Reports in Forensic Medical Science*. 5:67-74.

Isa, M.I., Fenton, T.W., Antonelli, L.S., Vaughan, P.E. & Wei, F. 2021. Investigating reverse butterfly fractures: An experimental approach and application of fractography. *Forensic Science International*. 325:110899.

Kemp, W.L. 2016. Postmortem change and its effect on evaluation of fractures. *Academy of Forensic Pathology*. 6(1):28-44.

Keys, K. & Ross, A.H. 2022. Identifying blunt force traumatic injury on thermally altered remains: a pilot study using *Sus scrofa*. *Biology*. 11(1):87.

Kimmerle, E.H & Baraybar, J.P. 2008. Skeletal trauma: *Identification of injuries resulting from human rights abuse and armed conflict.* Boca Raton: CRC Press.

Koch, S. & Lambert, J. 2017. Detection of skeletal trauma on whole pigs subjected to a fire environment. *Journal of Anthropology Reports*. 2(1):1–7.

Kooi, R. J. & Fairgrieve, S. I. 2013. SEM and stereomicroscopic analysis of cut marks in fresh and burned bone. *Journal of forensic sciences*. 58(2):452-458.

Krap, T., Duijst, W., Aalders, M.C. & Oostra, R.J. 2022. Mechanical or thermal damage: differentiating between underlying mechanisms as a cause of bone fractures. *International Journal of Legal Medicine*. 136(4):1133-1148.

Liebenberg, M., Liebenberg, L., Krüger, G.C. & L'Abbé, E.N. 2023. Veldt fires in South Africa: implications on osteometry and the biological profile. *Journal of Forensic Sciences*. 68:586-595.

Love, J.C., Derrick, S.M, Wiersema, J.M. & Peters, C. 2014. Microscopic saw mark analysis: an empirical approach. *Journal of Forensic Sciences*. 60(1):21-26.

Macoveciuc, I., Márquez-grant, N., Horsfall, I. & Zioupos, P. 2017. Sharp and blunt force trauma concealment by thermal alteration in homicides: An in-vitro experiment for methodology and protocol development in forensic anthropological analysis of burnt bones. *Forensic Science International.* 275:260–271. DOI: 10.1016/j.forsciint.2017.03.014.

Marciniak, S. 2008. Postmortem dismemberment and fire exposure: the identification of saw mark characteristics on burned bone. M.A. Thesis. Trent University.

Marciniak, S. 2009. A preliminary assessment of the identification of saw marks on burned bone. *Journal of Forensic Science*. 54(4):779-785.

Martlin, B. & Rando, C.R. 2020. An assessment of the reliability of cut surface characteristics to distinguish between hand-powered reciprocating saw blades in cases of experimental dismemberment. *Journal of Forensic Sciences*. 66:444-455.

Mata Tutor, P., Benito-Sánchez, M., Villoria-Rojas, C., Muñoz-García, A., Pérez-Guzmán, I. & Márquez-Grant, N. 2021a. Cut or burnt? – Categorizing morphological characteristics of heat-induced fractures and sharp force trauma. *Legal Medicine*. 50:101868. DOI: https://doi.org/10.1016/j.legalmed.2021.101868.

Mata-Tutor, P., Márquez-Grant, N., Villoria-Rojas, C., Muñoz-García, A., Pérez-Guzmán, I. & Benito-Sánchez, M. 2021b. Through fire and flames: post-burning survival and detection of dismemberment-related toolmarks in cremated cadavers. *International Journal of Legal Medicine*. 135(3):801-815.

Mata-Tutor, P., Villoria-Rojas, C., Márquez-Grant, N., Alvares de Buergo Ballester, M., Pérez-Ema, N. & Benito-Sánchez, M. 2022. Measuring dimensional and morphological heat alterations of dismemberment-related toolmarks with an optical roughness metre. *International Journal of Legal Medicine*. 136:343-356.

Moraitis, K. & Spiliopoulou, C. 2006. Identification and differential diagnosis of perimortem blunt force trauma in tubular long bones. *Forensic Science of Medical Pathology*. 2(4):221-229.

Nogueira, L., Quatrehomme, G., Rallon, C., Adalian, P. & Alunni, V. 2016. Saw marks in bones: A study of 170 experimental false start lesions. *Forensic Science International*. 268:123-130.

Nogueira, L., Alunni, V., Bernandi, C. & Quatrehomme, G. 2018. Saw marks in bones: A study of "secondary features" of false start lesions. *Forensic Science International*. 290:157-161.

Norman, D.G., Baier, W., Watson, D.G., Burnett, B., Painter, M. & Williams, M.A. 2018a. Micro-CT for saw mark analysis on human bone. *Forensic Science International*. 293:91-100.

Norman, D.G., Watson, D.G., Burnett, P.M. & Williams, M.A. 2018b. The cutting edge-Micro-CT for quantitative toolmark analysis of sharp force trauma. *Forensic Science International*. 283:156-172.

Pelletti, G., Viel, G., Fais, P., Viero, A., Visentin, S., Miotto, D., Montisci, M., Cecchetto, G. & Giraudo, C. 2017. Micro-computed tomography of false starts produced on bone by different hand-saws. *Legal Medicine*. 26:1-5.

Pope, E.J. & Smith, O.C. 2004. Identification of traumatic injury in burned cranial bone: an experimental approach. *Journal of Forensic Science*. 49(3):1-10.

Poppa, P., Porta, D., Gibelli, D., Mazzucchi, A., Brandone, A., Grandi, M. & Cattaneo, C. 2011. Detection of blunt, sharp force and gunshot lesions on burnt remains: a cautionary note. *The American Journal of Forensic Medicine and Pathology*. 32(3):275-279.

Reber, S.L. & Simmons, T. 2015. Interpreting injury mechanisms of blunt force trauma from butterfly fracture formation. *Journal of Forensic Sciences*. 60(6):1401–1411. DOI: 10.1111/1556-4029.12797.

Reichs, K.J. 1998. Postmortem dismemberment: recovery, analysis, and interpretation. In *Forensic osteology: advances in the identification of human remains*. C.C. Thomas, 2nd ed. Springfield. 353–88.

Robbins, S.C., Fairgrieve, S.I. & Oost, T.S. 2014. Interpreting the effects of burning on pre-incineration saw marks in bone. *Journal of Forensic Sciences*.
DOI: 10.1111/1556-4029.12580

Saville, P.A., Hainsworth, S.V. & Rutty, G.N. 2007. Cutting crime: the analysis of the "uniqueness" of saw marks on bone. *International Journal of Legal Medicine*. 121:349-357.

Shipman, P., Foster, G. & Schoeninger, M. 1984. Burnt bones and teeth: an experimental study of color, morphology, crystal structure and shrinkage. *Journal of Archaeological Sciences*. 11:307-325.

Symes, S.A. 1992. Morphology of saw marks in human bone: identification of class characteristics. PhD. Dissertation. University of Tennessee.

Symes, S.A. Rainwater, C.W., Chapman, E.N., Gipson, D.R. & Piper, A.L. 2008. Patterned thermal destruction in a forensic setting. In *The analysis of burned remains.* C.W. Schmidt & S.A. Symes, 2nd Eds. Amsterdam. Elsevier. 15-54.

Symes, S.A., Chapman, E.N., Rainwater, C.W., Cabo, L.L. & Myster, S.M.T. 2010. *Knife and saw toolmark analysis in bone: a manual designed for the examination of criminal mutilation and dismemberment.* (Research report 232864). Erie, Pennsylvania: Mercyhurst Archaeological institute, Mercyhurst College.

Symes, A.S., Dirkmaat, D.C., Ousley, S., Chapman, E. and Cabo, L. 2012. *Recovery and interpretation of burned human remains.* (Research report 237966). Erie, Pennsylvania: Mercyhurst Archaeological institute, Mercyhurst College.

Thompson, T.J.U. 2004. Recent advances in the study of burned bone and their implications for forensic anthropology. *Forensic Science International*. 146:S203-S205.

Thompson, T.J.U. 2005. Heat-induced dimensional changes in bone and their consequences for forensic anthropology. *Journal of Forensic Sciences*. 50:1008–1015. DOI: 10.1520/JFS2004297.

Thompson, T.J.U. & Inglis, J. 2009. Differentiation of serrated and non-serrated blades from stab marks in bone. *International Journal of Legal Medicine*. 123:129-135.

Thurman, M. & Willmore, L. 1980. A replicative cremation experiment. *North American Archaeologist*. 2:275-283.

Tümer, A.R., Akçan, R., Karacaoğlu, E., Balseven-Odabaşı, A., Keten, A., Kanburoğlu, Ç., Ünal, M. & Dinç, A.H. 2012. Postmortem burning of the corpses following homicide. *Journal of Forensic and Legal Medicine.* 19(4):223-228.

Ubelaker, D.H. 2009. The forensic evaluation of burned skeletal remains: A synthesis. *Forensic Science International.* 183(1-3):1-5.

Ubelaker, D.H. & Wu, Y. 2020. Fragment analysis in forensic anthropology. *Forensic Science Research*. 5(4):260-265.

Vachirawongsakorn, V., Painter, J. & Márquez-Grant, N. 2022. Knife cut marks inflicted by different blade types and the changes induced by heat: a dimensional and morphological study. *International Journal of Legal Medicine.* 136(1):329-342.

Van Niekerk, A., Laubscher, R. & Laflamme, L. 2009. Demographic and circumstantial accounts of burn mortality in Cape Town, South Africa, 2001-2004: An observation register based study. *BMC Public Health.* 9(374):1-10.

Vegh, E.I. & Rando, C. 2019. Effects of heat as a taphonomic agent on kerf dimensions. *Archeological and Environmental Forensic Science*. 1(2):105-118.

Waltenberger, L. & Schutkowski, H. 2017. Effects of heat on cut mark characteristics. *Forensic Science International.* 71:49-58.

Waterhouse, K. 2013. The effect of victim age on burnt bone fragmentation: Implications for remains recovery. *Forensic Science International*. 231(1-3):409.e1-409.e7.

Whyte, T. 2001. Distinguishing remains of human cremation from burned animal bones. *Journal of Field Archaeology.* 28(3-4):437-448.

Wieberg, D.A.M. & Wescott, D.J. 2008. Estimating the timing of long bone fractures: correlation between the post-mortem interval, bone moisture content, and blunt force trauma characteristics. *Journal of Forensic Sciences*. 53(5):1028-1034.

World Health Organisation. N.d. *Burns*. Available:

https://www.emro.who.int/health-topics/burns/index.html [2023, March 27].

World Health Organisation. 2018. *Burns, March 2018*. Available:

https://www.who.int/news-room/fact-sheets/detail/burns [2023, March 27].

APPENDIX A: Summary Table of Thermal Alteration on Pre-existing Trauma on Bone

Table A1: A summary of studies relating to thermal alteration on pre-existing trauma on bone.

Year	Author(s)	Burn type	Temperature (°C)	Duration	Bone species	Sample size	Cut type	Saw type
1999	Herrmann & Bennett	Outdoor fire	700°C - 850°C	2h30 min	Pig bone (*S. scrofa*)	12	Different depths of lesions and complete transections	a. Scalpel b. Knife c. Stryker saw d. Ripsaw
2004	Pope & Smith	Environments simulating forensic fires	204°C - 871°C	Not mentioned	Unembalmed human heads	6	a. Incisions b. Cut marks c. Chop marks d. Full transections	a. Scalpel b. Knife c. Autopsy saw
2009	Marciniak	Outdoor fire	>800°C	3 hrs	Semi-fleshed pig femur bones (*S. scrofa*)	36	False starts	a. Handsaws b. Power saws
2011	Poppa et al.	Iron grill on gas cookers	Not mentioned (underwent calcination)	Not mentioned	Pig heads	9 (27 lesions)	Lesions	a. Saw b. Hatchet c. Star-shaped screwdriver
2012	Symes	Furnace	500°C	~90 min	a. Human humeri & femora b. Pig (*S.scrofa*) limbs bones	a. 19 human b. 24 pig	Bone sections and kerfs a. 7 human bone sections b. 25 pig bone sections	Handsaws (alternating)
2013	Kooi & Fairgrieve	Outdoor fire pit	Not mentioned	1 hr	Semi-fleshed pig rib bones (*S. scrofa*)	Not mentioned	Stab and cut marks	Kitchen knives: a. smooth b. serrated edge
2014	Robbins	Outdoor fire pit	710°C - 720°C	3 hrs	Semi-fleshed pig long bones (*S.scrofa*)	24	Deep and shallow false starts and bone sections	a. Hacksaw (wavy) b. Back saw (alternating) c. PVC saw (alternating) d. Universal (alternating) saw e. Aggressive saw (alternating) f. Course cut carpenter saw (alternating) g. Drywall saw (alternating & raker)
2017	Koch & Lambert	Indoor: burn cell	a. ~600°C b. ~1000°C	-8 min -22.5 min	Pig carcasses (*S. scrofa*)	6	Stab and cut marks	Knife

2017	Macovecuic et al.	Electric furnace	820°C	58 min	Juvenile sheep radii	7	Cut marks	Test rig with sharp blade (mimics large knife)
2017	Waltenberger & Scutkowski	Electric furnace	700°C	3 hrs	Juvenile pig ribs (*S.scrofa*)	9 (11 cut marks)	Cut marks (false starts)	Cooking knives: a. straight & non-serrated b. slightly curved c. strongly curved upwards
2018	Alunni et al.	Outdoor wooden pyre)	400°C-700°C	10 min	De-fleshed pig femurs	4 bones (30 lesions)	False start	Hatchet
2019	Vegh & Rando	Electric furnace	a. 300°C b. 600°C c. 800°C d. 1000°C	20 min	De-fleshed pig ribs (*S.scrofa*)	16	False starts	a. Kitchen knife (non-serrated) b. Hacksaw (wavy) c. Wood saw (alternating)
2020	Collord-Stalder	Outdoor grill	(-)200°C -1200°C	1h45min - 2h57min	a. Pig bones (*S. scrofa*) b. Human bones	54 bones (216 lesions both)	Incomplete lesions	a. Knives (serrated & non-serrated) b. Reciprocating power saw c. Handsaw
2021	Mata-Tutor et al.	Crematorium furnace	701°C	85 min	Embalmed human cadavers	3	a. Chop marks b. Cut marks	a. Machete c. Serrated bread knife
2022	Keys & Ross	Outdoor fire	Until calcined	1h40min	Fleshed pig skulls (*S. scrofa*)	11	Blunt force	a. Crowbar b. Hammer
2022	Krap et al.	Indoor: concrete firehouse	700°C -800°C	50 min	Human cadaveric radii	30	Blunt force	Custom made pendulum (mimics baseball bat)
2022	Mata-Tutor et al.	Chamber furnace	39°C -850°C	30 min	De-fleshed juvenile pig femur and tibia bones	4 (120 lesions)	a. False starts b. Chop marks c. Cut marks (Different depths)	a. Serrated bread knife b. Buthcer machete c. Saw
2022	Vachirawongsakorn et al.	Electric furnace	850°C	30 min	De-fleshed pig ribs (*S.scrofa*)	240	Cut marks	Knives: a. serrated b. non-serrated c. course serrated

APPENDIX B: Bone Biomechanics Measurements

In order to group the bones according to the formula, biomechanical measurements were recorded. This includes measuring the anterior-posterior (AP) width, the medial-lateral (ML) width and the length of each bone. Once the moment of inertia (I) value was calculated, bones were distributed evenly across the controlled temperatures (400°C, 600°C and 800°C). A digital calliper was used to measure the AP, ML and length of the bone samples.

Moment of inertia: The ability of bone to resist bending.

$$I = \frac{\pi d^4}{64}$$

Table B1: Biomechanical measurements of bones.

Sample Identification	AP (mm)	I AP (mm⁴)	ML (mm)	I ML (mm⁴)	Length (mm)
S1-a	20.00	7853.98	18.61	5887.83	108.10
S2-a	21.07	9674.49	18.00	5153.00	98.99
S3-a	19.17	6629.16	18.68	5976.92	89.08
S4-a	20.86	9294.52	18.94	6316.69	99.09
S5-a	19.60	7244.26	17.50	4603.86	94.05
S6-a	20.48	8635.54	19.53	7141.33	92.60
S7-b	20.35	8418.36	19.61	7259.06	88.18
S8-b	20.36	8434.92	19.47	7053.97	80.24
S9-b	20.14	8076.21	18.03	5187.44	91.49
S10-b	21.40	8501.42	18.58	5849.96	90.48
S11-b	17.71	4828.85	18.21	5397.71	93.21
S12-b	19.26	6754.53	19.52	7126.71	92.64
S13-c	20.17	8124.44	18.98	6370.22	86.82
S14-c	29.59	37631.35	27.48	27992.19	109.93
S15-c	27.79	29276.83	30.28	41813.93	118.83
S16-c	22.47	12513.60	21.43	10352.82	110.35
S17-c	23.43	14793.10	22.73	13102.91	110.87
S18-c	21.61	10705.06	20.83	9241.17	116.63

*Sample identification was re-labelled when bones were distributed in the three temperature groups.

APPENDIX C: Ethics Approval Letter

UNIVERSITY OF CAPE TOWN
Faculty of Health Sciences
Animal Ethics Committee

Room G50 Old Main Building
Groote Schuur Hospital
Observatory 7925
Website: www.health.uct.ac.za/fhs/research/animalethics/forms

25 July 2022

Mr Calvin Mole
Division of Forensic Medicine and Toxicology
Department of Pathology
Faculty of Health Sciences
University of Cape Town

Dear Mr Mole

PROTOCOL TITLE: ***The Effect of Burning on Pre-incineration Trauma in Bone***

FHS AEC REF NO: 022_015

Thank you for submitting your amended protocol to the Faculty of Health Sciences (FHS) Animal Ethics Committee (AEC) for review.

I am pleased to inform you that the FHS AEC has **authorised** your protocol, which will terminate on **31 July 2025.**

Number of animals & species:

- 145 Sheep bones (femurs)

Please quote the FHS AEC REF NO (above) in all future correspondence.

Please note that the authorisation of this protocol imposes the following obligations on the principal investigator (PI):

1. To submit an annual mandatory progress report. The first annual report for this protocol is due on **28 February 2023**. The forms can be accessed from http://www.health.uct.ac.za/fhs/research/animalethics/forms
2. To submit a final mandatory report on the **31 July 2025**, please access the final report form from: http://www.health.uct.ac.za/fhs/research/animalethics/forms
3. Ensuring that all study participants perform within the confines of the procedures and experimental design of the protocol as authorised, or as amended.

4. Ensuring that all study participants comply with all applicable national legislation, UCT policies, FHS AEC policies and standard operating procedures (SOPs) and national standards (SANS 10386: 2008).
5. Ensuring compliance with DAFF Section 20 requirements.
6. Ensuring that you as the PI immediately alert the FHS AEC to any event involving the welfare of the animals which has occurred during the course of the study, as well as the actions that were taken to respond to these events.
7. Ensuring that you as the PI alert the FHS AEC to any new or unexpected ethical issues that arose during the course of the study, and how these issues were addressed.
8. Ensuring that all study participants are registered with or have been authorised by the South African Veterinary Council (SAVC) to perform the procedures on animals or will be performing the procedures under the direct and continuous supervision of SAVC-registered veterinary professionals or SAVC-registered para-veterinary professionals.
9. If the PI or any study participant is in any way uncertain how to respond to any of these obligations or deal with any of the issues referred to above, they must consult with FHS AEC.
10. All animals found dead must be reported to the RAF on the appropriate form: http://www.health.uct.ac.za/fhs/research/animalethics/forms
11. All animals found in distress must be reported to the RAF on the appropriate form.

My best wishes for successful research and /or teaching endeavour.

Yours sincerely

PROF G. LOUW
CHAIR, FHS AEC

AEC REF# 022_015

APPENDIX D: Heat-induced Fractures and Colouration of Bones

Table D1: Number of fracture types and colour (Adapted from Symes and colleagues, 2008).

	Sample identification																	
	S1-a	*S2-a*	*S3-a*	*S4-a*	*S5-a*	*S6-a*	*S7-b*	*S8-b*	*S9-b*	*S10-b*	*S11-b*	*S12-b*	*S13-c*	*S14-c*	*S15-c*	*S16-c*	*S17-c*	*S18-c*
	400°C						**600°C**						**800°C**					
Fracture type	**Number of fractures (Presence)**																	
Longitudinal fracture	3	3	3	2	4	5	1	3	3	5	3	3	None	5	10	None	11	7
Step fracture	None	1	None	1	None	None	None	None	None	1	None	2	3	None	2	2	2	6
Transverse fracture	None	1	None	1	1	None	1	1	1	2	None	None	1	None	4	3	3	5
Curved transverse fracture	None	2	None	1	None	2	None	3	None	5	None	1	3	1	4	2	2	7
Patina fractures	None	None	None	None	None	None	None	None	None	None	None	None	None	None	None	None	Multiple	Multiple
Delamination & Splintering fractures	Minimal	Minimal	Minimal - Intermediate	Minimal	None	Intermediate	None	Minimal	Minimal	Minimal	Intermediate	Intermediate	Multiple	Multiple	Multiple	Intermediate	Intermediate	Multiple
Heat line fracture	None	None	None	None	None	None	None	None	None	None	None	None	None	None	None	None	None	None
Colour	Black/charred	Black/charred	Black/charred	Black/charred	Brown-black/charred	Brown-black/charred	Black-Grey/charred	Black-Grey-white/charred	Black-Grey/charred	Black-Grey/charred	Black-blue/charred	Black-Blue-Grey/charred	Blue-White-Grey	Black - Grey-White	Black - White-Grey	Blue-Black,Grey-white	Blue-Grey-White	Grey(chalky), Blue-white

APPENDIX E: Bone Weight Before and After Burning

Table E1: Bone weight before and after burning.

Sample identification	Temperature group	Pre-burning weight (g)	Post-burning weight (g)
S1-a	400°C	184.6	96.3
S2-a		180.9	106.5
S3-a		177.8	85.1
S4-a		168.7	81.4
S5-a		125.5	66.3
S6-a		184.8	45.9
S7-b	600°C	176.3	70.0
S8-b		180.0	75.8
S9-b		165.1	67.7
S10-b		180.5	70.2
S11-b		164.5	92.1
S12-b		186.2	77.1
S13-c	800°C	176.6	62.9
S14-c		209.5	60.3
S15-c		211.6	59.9
S16-c		208.3	74.9
S17-c		195.7	62.1
S18-c		130.1	60.5

APPENDIX F: Additional Visualisation Methods

F1. Silicone casting method

a. Spray release agent on the saw mark where casts will be applied on.

b. Weigh equal parts of Part A (blue) and Part B (pink) in separate containers on the analytical balance scale.

c. Pour Part B into Part A (make sure Part B container is scraped as clean as possible).

d. Mix approximately for 2 minutes (fold rather than whipping to avoid air bubbles).

e. Place the bones on the steel tray to catch any drips.

f. Once casting solution is ready, use syringe to pour on the saw marks (false starts and incomplete cuts) in a continuous motion.

g. Use spoon to pour onto complete transections.

h. Add extra to ensure cast is not too thin.

i. Allow to dry open air for minimum 20 minutes or overnight for better texture and stability.

j. Once dry, carefully peel off and analyse.

k. Casts can be stored in a plastic container in room temperature.

Figure F1: Casts applied onto the false start lesions, incomplete cuts and complete transection on fresh bones.

F2. Fingerprint powder method

a. Pour black fingerprint powder onto a lid.

b. Use a brush and lightly dab to pick up the powder. If too much lightly tap the brush stick to shake off excess.

c. Lightly and gently brush onto the target surface (complete transections) until surface area is covered enough.

d. Analyse and photograph the surface area.

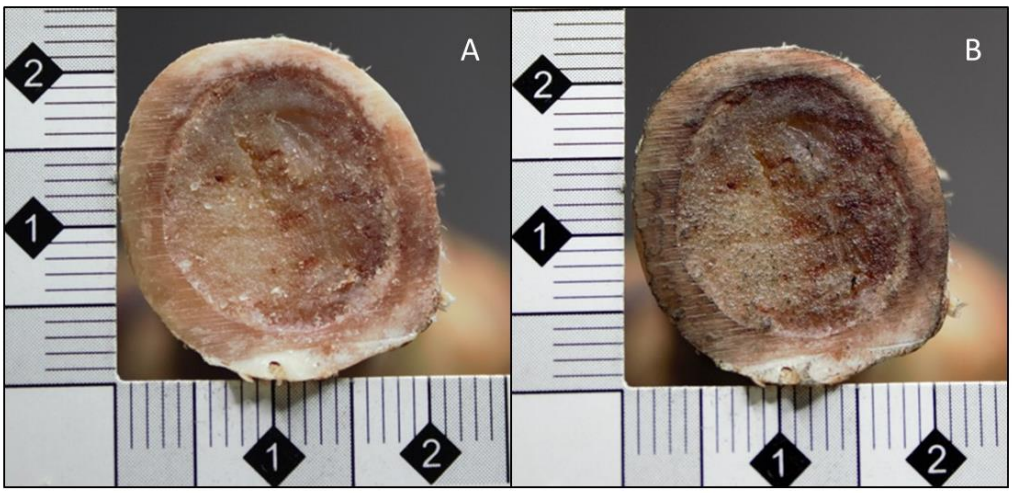

Figure F2: Black fingerprint powder applied to enhance striations on cut surface. A) Complete transection surface without fingerprint powder and B) fingerprint powder applied.

APPENDIX G: Measurements of Saw Mark Characteristics

Table G1: Measurements of different cut types from specimen 1 pre- and post-burning.

Specimen 1 (S1-a)	Cut Types	Pre-burning	Post-burning (400°C)
Average kerf width	False starts	1,10 mm	1,13 mm
Maximum kerf depth		1,14 mm	0,84 mm
Average kerf width	Incomplete cuts	1,16 mm	1,24 mm
Maximum kerf depth		6,14 mm	6,61 mm
Breakaway spur max thickness	Complete transection (Cut surface 1)	0,87 mm	0,8 mm
Breakaway spur max length		0,46 mm	0,64 mm
Pull-out striae average distance		0 mm	0 mm
Average distance between striae		0,09 mm	0,09 mm
Breakaway spur max thickness	Complete transection (Cut surface 2)	1,11 mm	1 mm
Breakaway spur max length		0,43 mm	0,63 mm
Pull-out striae average distance		0 mm	0 mm
Average distance between striae		0,085 mm	0,079 mm

Table G2: Measurements of different cut types from specimen 2 pre- and post-burning.

Specimen 2 (S2-a)	Cut Types	Pre-burning	Post-burning (400°C)
Average kerf width	False starts	0,89 mm	1,22 mm
Maximum kerf depth		0,63 mm	0,75 mm
Average kerf width	Incomplete cuts	1,14 mm	1,43 mm
Maximum kerf depth		5,64 mm	6,23 mm
Breakaway spur max thickness	Complete transection (Cut surface 1)	1,42 mm	1,33 mm
Breakaway spur max length		1,10 mm	1,33 mm
Pull-out striae average distance		0,735 mm	1 mm
Average distance between striae		0,085 mm	0,067 mm
Breakaway spur max thickness	Complete transection (Cut surface 2)	1,61 mm	1,37 mm
Breakaway spur max length		1,07 mm	1,54 mm
Pull-out striae average distance		0 mm	0 mm
Average distance between striae		0,1017 mm	0,061 mm

Table G3: Measurements of different cut types from specimen 3 pre- and post-burning.

Specimen 3 (S3-a)	Cut Types	Pre-burning	Post-burning (400°C)
Average kerf width	False starts	0,96 mm	1,09 mm
Maximum kerf depth		0,94 mm	0,74 mm
Average kerf width	Incomplete cuts	1,16 mm	1,1 mm
Maximum kerf depth		3,01 mm	3,32 mm
Breakaway spur max thickness	Complete transection (Cut surface 1)	2,28 mm	1,88 mm
Breakaway spur max length		2,29 mm	1,49 mm
Pull-out striae average distance		0 mm	0 mm
Average distance between striae		0,1117 mm	0,072 mm
Breakaway spur max thickness	Complete transection (Cut surface 2)	2,19 mm	1,95 mm
Breakaway spur max length		1,49 mm	1,32 mm
Pull-out striae average distance		0 mm	0 mm
Average distance between striae		0,1017 mm	0,063 mm

Table G4: Measurements of different cut types from specimen 4 pre- and post-burning.

Specimen 4 (S4-a)	Cut Types	Pre-burning	Post-burning (400°C)
Average kerf width	False starts	0,7 mm	1,21 mm
Maximum kerf depth		0,62 mm	0,67 mm
Average kerf width	Incomplete cuts	1,15 mm	1,11 mm
Maximum kerf depth		4,62 mm	5,28 mm
Breakaway spur max thickness	Complete transection (Cut surface 1)	1,77 mm	1,57 mm
Breakaway spur max length		1,01 mm	1,2 mm
Pull-out striae average distance		0 mm	0 mm
Average distance between striae		0,1167 mm	0,06 mm
Breakaway spur max thickness	Complete transection (Cut surface 2)	2,07 mm	1,78 mm
Breakaway spur max length		1,44 mm	1,35 mm
Pull-out striae average distance		0 mm	0 mm
Average distance between striae		0,0667 mm	0,056 mm

Table G5: Measurements of different cut types from specimen 5 pre- and post-burning.

Specimen 5 (S5-a)	Cut Types	Pre-burning	Post-burning (400°C)
Average kerf width	False starts	1,33 mm	1,21 mm
Maximum kerf depth		0,64 mm	0,86 mm
Average kerf width	Incomplete cuts	1,16 mm	1,09 mm
Maximum kerf depth		3,76 mm	3,76 mm
Breakaway spur max thickness	Complete transection (Cut surface 1)	2,57 mm	1,95 mm
Breakaway spur max length		2,94 mm	3,03 mm
Pull-out striae average distance		0,07 mm	0,995 mm
Average distance between striae		0,095 mm	0,05 mm
Breakaway spur max thickness	Complete transection (Cut surface 2)	0,58 mm	0,77 mm
Breakaway spur max length		1,08 mm	0,95 mm
Pull-out striae average distance		0 mm	0.034 mm
Average distance between striae		0,1017 mm	0,04 mm

Table G6: Measurements of different cut types from specimen 6 pre- and post-burning.

Specimen 6 (S6-a)	Cut Types	Pre-burning	Post-burning (400°C)
Average kerf width	False starts	1,15 mm	1,54 mm
Maximum kerf depth		1,08 mm	0,89 mm
Average kerf width	Incomplete cuts	1,13 mm	N/A
Maximum kerf depth		8,66 mm	7,2 mm
Breakaway spur max thickness	Complete transection (Cut surface 1)	1,23 mm	0 mm
Breakaway spur max length		0,32 mm	0 mm
Pull-out striae average distance		0 mm	0 mm
Average distance between striae		0,0733 mm	0,057 mm
Breakaway spur max thickness	Complete transection (Cut surface 2)	1,92 mm	1,63 mm
Breakaway spur max length		1,14 mm	1,57 mm
Pull-out striae average distance		0 mm	0 mm
Average distance between striae		0,0567 mm	0,039 mm

Table G7: Measurements of different cut types from specimen 7 pre- and post-burning

Specimen 7 (S7-b)	Cut Types	Pre-burning	Post-burning (600°C)
Average kerf width	False starts	0,83 mm	1,23 mm
Maximum kerf depth		0,83 mm	0,62 mm
Average kerf width	Incomplete cuts	1,13 mm	1,16 mm
Maximum kerf depth		5,85 mm	6,95 mm
Breakaway spur max thickness	Complete transection (Cut surface 1)	1,78 mm	1,54 mm
Breakaway spur max length		1,79 mm	1,08 mm
Pull-out striae average distance		0 mm	0 mm
Average distance between striae		0,09 mm	0,037 mm
Breakaway spur max thickness	Complete transection (Cut surface 2)	1,13 mm	1,27 mm
Breakaway spur max length		0,91 mm	1,41 mm
Pull-out striae average distance		0 mm	0 mm
Average distance between striae		0,0667 mm	0,048 mm

Table G8: Measurements of different cut types from specimen 8 pre- and post-burning.

Specimen 8 (S8-b)	Cut Types	Pre-burning	Post-burning (600°C)
Average kerf width	False starts	0,64 mm	1,14 mm
Maximum kerf depth		0,76 mm	0,56 mm
Average kerf width	Incomplete cuts	1,20 mm	1,15 mm
Maximum kerf depth		2,89 mm	2,85 mm
Breakaway spur max thickness	Complete transection (Cut surface 1)	1,22 mm	0,72 mm
Breakaway spur max length		0,85 mm	0,55 mm
Pull-out striae average distance		0 mm	0 mm
Average distance between striae		0,09 mm	0,057 mm
Breakaway spur max thickness	Complete transection (Cut surface 2)	1,50 mm	1,36 mm
Breakaway spur max length		1,20 mm	1,03 mm
Pull-out striae average distance		0 mm	0 mm
Average distance between striae		0,08 mm	0,04 mm

Table G9: Measurements of different cut types from specimen 9 pre- and post-burning.

Specimen 9 (S9-b)	Cut Types	Pre-burning	Post-burning (600°C)
Average kerf width	False starts	0,74 mm	1,19 mm
Maximum kerf depth		0,57 mm	0,76 mm
Average kerf width	Incomplete cuts	1,16 mm	1,14 mm
Maximum kerf depth		3,4 mm	3,5 mm
Breakaway spur max thickness	Complete transection (Cut surface 1)	1,53 mm	1,53 mm
Breakaway spur max length		1,77 mm	1,38 mm
Pull-out striae average distance		0 mm	0 mm
Average distance between striae		0,0767 mm	0,059 mm
Breakaway spur max thickness	Complete transection (Cut surface 2)	1,73 mm	1,8 mm
Breakaway spur max length		0,87 mm	0,85 mm
Pull-out striae average distance		0 mm	0 mm
Average distance between striae		0,1083 mm	0,059 mm

Table G10: Measurements of different cut types from specimen 10 pre- and post-burning.

Specimen 10 (S10-b)	Cut Types	Pre-burning	Post-burning (600°C)
Average kerf width	False starts	1,16 mm	1,26 mm
Maximum kerf depth		0,72 mm	0,98 mm
Average kerf width	Incomplete cuts	1,16 mm	1,21 mm
Maximum kerf depth		5,35 mm	4,71 mm
Breakaway spur max thickness	Complete transection (Cut surface 1)	2,01 mm	1,61 mm
Breakaway spur max length		0,27 mm	0,5 mm
Pull-out striae average distance		0 mm	0 mm
Average distance between striae		0,08 mm	0,088 mm
Breakaway spur max thickness	Complete transection (Cut surface 2)	2,03 mm	2,11 mm
Breakaway spur max length		0,93 mm	1,69 mm
Pull-out striae average distance		0 mm	0 mm
Average distance between striae		0,0683 mm	0,037 mm

Table G11: Measurements of different cut types from specimen 11 pre- and post-burning.

Specimen 11 (S11-b)	Cut Types	Pre-burning	Post-burning (600°C)
Average kerf width	False starts	1,09 mm	1,40 mm
Maximum kerf depth		0,76 mm	0,62 mm
Average kerf width	Incomplete cuts	1,16 mm	1,04 mm
Maximum kerf depth		6,53 mm	6,19 mm
Breakaway spur max thickness	Complete transection (Cut surface 1)	1,3 mm	1,31 mm
Breakaway spur max length		0,92 mm	0,93 mm
Pull-out striae average distance		0,7 mm	0 mm
Average distance between striae		0,1033 mm	0,048 mm
Breakaway spur max thickness	Complete transection (Cut surface 2)	1,35 mm	1,27 mm
Breakaway spur max length		0,97 mm	1,15 mm
Pull-out striae average distance		0 mm	0 mm
Average distance between striae		0,08 mm	0,071 mm

Table G12: Measurements of different cut types from specimen 12 pre- and post-burning.

Specimen 12 (S12-b)	Cut Types	Pre-burning	Post-burning (600°C)
Average kerf width	False starts	0,84 mm	0,90 mm
Maximum kerf depth		0,75 mm	0,63 mm
Average kerf width	Incomplete cuts	1,08 mm	1,20 mm
Maximum kerf depth		5,69 mm	6,09 mm
Breakaway spur max thickness	Complete transection (Cut surface 1)	2,02 mm	2,04 mm
Breakaway spur max length		3,90 mm	2,50 mm
Pull-out striae average distance		0 mm	0 mm
Average distance between striae		0,0967 mm	0,053 mm
Breakaway spur max thickness	Complete transection (Cut surface 2)	1,58 mm	1,94 mm
Breakaway spur max length		0,82 mm	1,68 mm
Pull-out striae average distance		0 mm	0 mm
Average distance between striae		0,0817 mm	0,066 mm

Table G13: Measurements of different cut types from specimen 13 pre- and post-burning.

Specimen 13 (S13-c)	Cut Types	Pre-burning	Post-burning (800°C)
Average kerf width	False starts	1,31 mm	1,38 mm
Maximum kerf depth		0,78 mm	N/A
Average kerf width	Incomplete cuts	1,16 mm	1,25 mm
Maximum kerf depth		3,3 mm	2,74 mm
Breakaway spur max thickness	Complete transection (Cut surface 1)	1,78 mm	0,58 mm
Breakaway spur max length		1,71 mm	0,41 mm
Pull-out striae average distance		0 mm	0.179 mm
Average distance between striae		0,0917 mm	0,057 mm
Breakaway spur max thickness	Complete transection (Cut surface 2)	1,84 mm	1,72 mm
Breakaway spur max length		0,69 mm	0,99 mm
Pull-out striae average distance		0 mm	0 mm
Average distance between striae		0,0817 mm	0,054 mm

Table G14: Measurements of different cut types from specimen 14 pre- and post-burning.

Specimen 14 (S14-c)	Cut Types	Pre-burning	Post-burning (800°C)
Average kerf width	False starts	1,22 mm	1,35 mm
Maximum kerf depth		0,72 mm	N/A
Average kerf width	Incomplete cuts	1,19 mm	1,43 mm
Maximum kerf depth		3,69 mm	3,69 mm
Breakaway spur max thickness	Complete transection (Cut surface 1)	2,1 mm	0,74 mm
Breakaway spur max length		0,56 mm	0,56 mm
Pull-out striae average distance		0.04 mm	0 mm
Average distance between striae		0,0833 mm	0,057 mm
Breakaway spur max thickness	Complete transection (Cut surface 2)	2,18 mm	2,04 mm
Breakaway spur max length		1,2 mm	1,45 mm
Pull-out striae average distance		0 mm	0 mm
Average distance between striae		0,1167 mm	0,056 mm

Table G15: Measurements of different cut types from specimen 15 pre- and post-burning.

Specimen 15 (S15-c)	Cut Types	Pre-burning	Post-burning (800°C)
Average kerf width	False starts	1,44 mm	0 mm
Maximum kerf depth		0,77 mm	N/A
Average kerf width	Incomplete cuts	1,22 mm	1,44 mm
Maximum kerf depth		3,25 mm	3,09 mm
Breakaway spur max thickness	Complete transection (Cut surface 1)	2 mm	0,59 mm
Breakaway spur max length		1,03 mm	0,66 mm
Pull-out striae average distance		0 mm	0 mm
Average distance between striae		0,11 mm	0,069 mm
Breakaway spur max thickness	Complete transection (Cut surface 2)	1,8 mm	1,24 mm
Breakaway spur max length		1,43 mm	1,57 mm
Pull-out striae average distance		0 mm	0 mm
Average distance between striae		0,1033 mm	0,059 mm

Table G16: Measurements of different cut types from specimen 16 pre- and post-burning.

Specimen 16 (S16-c)	Cut Types	Pre-burning	Post-burning (800°C)
Average kerf width	False starts	1,12 mm	1,16 mm
Maximum kerf depth		0,78 mm	0,5 mm
Average kerf width	Incomplete cuts	4,16 mm	4,18 mm
Maximum kerf depth		4,16 mm	4,18 mm
Breakaway spur max thickness	Complete transection (Cut surface 1)	1,6 mm	0,98 mm
Breakaway spur max length		1,08 mm	1,29 mm
Pull-out striae average distance		0 mm	0 mm
Average distance between striae		0,07 mm	0,053 mm
Breakaway spur max thickness	Complete transection (Cut surface 2)	1,78 mm	0,22 mm
Breakaway spur max length		1,19 mm	0,76 mm
Pull-out striae average distance		0 mm	0 mm
Average distance between striae		0,0617 mm	0,039 mm

Table G17: Measurements of different cut types from specimen 17 pre- and post-burning.

Specimen 17 (S17-c)	Cut Types	Pre-burning	Post-burning (800°C)
Average kerf width	False starts	1,25 mm	0,79 mm
Maximum kerf depth		0,9 mm	N/A
Average kerf width	Incomplete cuts	1,13 mm	1,3 mm
Maximum kerf depth		3,48 mm	2,92 mm
Breakaway spur max thickness	Complete transection (Cut surface 1)	1,58 mm	1,45 mm
Breakaway spur max length		0,81 mm	1,33 mm
Pull-out striae average distance		0 mm	0 mm
Average distance between striae		0,0667 mm	0,068 mm
Breakaway spur max thickness	Complete transection (Cut surface 2)	1,66 mm	1,4 mm
Breakaway spur max length		1,3 mm	1,67 mm
Pull-out striae average distance		0 mm	0 mm
Average distance between striae		0,09 mm	0,052 mm

Table G18: Measurements of different cut types from specimen 18 pre- and post-burning.

Specimen 18 (S18-c)	Cut Types	Pre-burning	Post-burning (800°C)
Average kerf width	False starts	1,16 mm	0,82 mm
Maximum kerf depth		0,78 mm	N/A
Average kerf width	Incomplete cuts	1,21 mm	1,42 mm
Maximum kerf depth		3,66 mm	3,06 mm
Breakaway spur max thickness	Complete transection (Cut surface 1)	1,81 mm	1,29 mm
Breakaway spur max length		0,56 mm	0,62 mm
Pull-out striae average distance		0 mm	0 mm
Average distance between striae		0,085 mm	0,065 mm
Breakaway spur max thickness	Complete transection (Cut surface 2)	1,78 mm	1,44 mm
Breakaway spur max length		0,92 mm	1,39 mm
Pull-out striae average distance		0,43 mm	0,27 mm
Average distance between striae		0,0717 mm	0,057 mm

APPENDIX H: Saw Mark Data Collection (Meta-data)

Table H1: List of variables collected and coding of saw mark characteristics.

Characteristic	Collected from	Code
Average kerf depth	-False start -Incomplete cut	Numerical value (Continuous)
Average Kerf width	False start Incomplete cut	Numerical value (Continuous)
Blade drift	False Start	Presence/Absence 1 = yes, 0 = no
Bone island	False Start	Presence/Absence 1 = yes, 0 = no
Breakaway spur	Complete transections	Presence/Absence 1 = yes, 0 = no
Breakaway spur length	Complete transections	Numerical value (Continuous)
Breakaway spur thickness	Complete transections	Numerical value (Continuous)
Exit chipping	-Incomplete cut -Complete transection (Cut surface 1 & 2)	Presence/Absence 1 = yes, 0 = no
Harmonics	-Incomplete cut -Complete transection (Cut surface 1 & 2)	Presence/Absence 1 = yes, 0 = no
Profile shape	-False Start -Incomplete cut	1 = Round 2 = Square 3 = Square with round corners 4 = V-shape 5 = W-shape 6 = W-truncated (Adapted from Nogeira et al., 2016)
Pull-out Striae	Complete transection (Cut surface 1 & 2)	Presence/Absence 1 = yes, 0 = no
Pull-out Striae amount	Complete transection (Cut surface 1 & 2)	Numerical value (discrete)
Average distance between striations	Complete transection (Cut surface 1 & 2)	Numerical value (Continuous)
Striation regularity	Complete transection (Cut surface 1 & 2)	1 = Uniform 0 = Non-uniform
Shape of the kerf wall	-False Start -Incomplete cut	1 = Narrow & wide 2 = Straight 3 = Necking
Tooth hop	Complete transection (Cut surface 1 & 2)	Presence/Absence 1 = yes, 0 = no
Tooth hop amount	Complete transection (Cut surface 1 & 2)	Numerical value (discrete)